Unified Analysis of UWB Transmitted-Reference Schemes in the Presence of Narrowband Interference

Tony Q. S. Quek, *Student Member, IEEE,* Moe Z. Win, *Fellow, IEEE* and Davide Dardari, *Member, IEEE*

***Abstract*— Transmitted-Reference (TR) signaling, in conjunction with an autocorrelation receiver (AcR), offers a low-complexity alternative to Rake reception in ultrawide bandwidth systems. This paper provides a unified performance analysis of various TR schemes by developing an analytical framework based on the sampling expansion approach. Specifically, we derive the uncoded bit error probability (BEP) of different TR signaling schemes, including TR and differential TR (DTR) signaling valid for a broad class of fading channels. We consider both AcRs and modified AcRs with noise averaging. We further develop a quasi-analytical method as well as an approximate analytical method to extend the BEP analysis to include the effect of narrowband interference (NBI). We show that the approximate analytical method is particularly useful in obtaining BEP expressions that provide insight into the effect of NBI. We quantify the effects of NBI and channel power dispersion profile on the optimum integration interval of an AcR. Finally, we compare TR and DTR signaling in terms of their sensitivity to NBI.**

***Index Terms*— Ultrawide bandwidth systems, transmitted-reference, differential transmitted-reference, sampling expansion, narrowband interference.**

I. Introduction

RECENTLY, there has been a renewed interest in utilizing ultrawide bandwidth (UWB) spread-spectrum communications for future military, homeland security, and commercial applications [1]–[4]. UWB systems involve transmission of a train of extremely narrow pulses by employing either time-hopping (TH) or direct sequence (DS) techniques for multiple-access and pulse position modulation (PPM) or pulse amplitude modulation (PAM) for data transmission [1], [2]. The key motivation for using UWB systems is the ability to highly resolve multipath, as well as the availability of technology to implement and generate UWB signals with relatively low complexity. The fine delay resolution properties make UWB radio a viable candidate for communications [5]–[8], as well as for ranging and localization in dense multipath environments [9]–[14].

Due to its large transmission bandwidth, UWB systems need to coexist and contend with many narrowband communication systems. Therefore, a thorough performance analysis of such systems in the presence of narrowband systems is essential for successful deployment of UWB systems. Previous work in this area includes the study of the effect of UWB signals on some commercial narrowband communication systems [15]–[18], the analysis of UWB systems in the presence of narrowband interference (NBI) with conventional receiver structures involving a locally generated reference (LGR) [19]–[25], and the development of techniques to suppress NBI in UWB systems [26]–[30].

As an alternative to LGR systems, a reference signal can be transmitted along with the data. Such a signaling scheme, referred to as transmitted-reference (TR) signaling, was first considered in the early 1950s [31]. TR signaling involves the transmission of a reference and data signal pair, separated either in time [32], [33] or in frequency [34], [35].[1] Due to its simplicity, there is renewed interest in TR signaling for UWB systems [36]–[40], which can exploit multipath diversity inherent in the environment without the need for channel estimation and stringent acquisition [41]–[44]. The receiver can simply be an autocorrelation receiver (AcR), which can be modified to include noise averaging for better performance. Since TR signaling allocates a significant part of the symbol energy to transmitting reference pulses, differential encoding over consecutive symbols can also be used to alleviate inefficient resource usage. This alternative TR signaling is referred to as differential transmitted-reference (DTR) signaling [45], [46]. However, only a few results are available for the performance of TR and DTR signaling schemes in the presence of NBI [47]–[49].

In this paper, we analyze the performance of TR and DTR signaling schemes in the presence of NBI. We adopt the sampling expansion approach, originally proposed in [38], [39] to analyze TR schemes. First, we derive the uncoded BEP for TR and DTR signaling when an AcR or a modified AcR is used in a broad class of dense multipath channels

Manuscript received October 3, 2005; revised September 17, 2006; accepted September 24, 2006. The associate editor coordinating the review of this paper and approving it for publication was X. Shen. This research was supported, in part, by the Charles Stark Draper Laboratory Robust Distributed Sensor Networks Program, the Office of Naval Research Young Investigator Award N00014-03-1-0489, the National Science Foundation under Grants ANI-0335256 and ECS-0636519, DoCoMo USA Labs, Ministero dell'Istruzione, Università e della Ricerca Scientifica (MIUR) under the VICOM Project, Italy, and the Institute of Advanced Study Natural Science & Technology Fellowship. Tony Q. S. Quek was supported in part by the ASTAR National Science Scholarship. This paper was presented in part at the IEEE International Conference on Ultra-Wideband, Zurich, Switzerland, September 2005.

Tony Q. S. Quek and Moe Z. Win are with the Laboratory for Information & Decision Systems (LIDS), Massachusetts Institute of Technology, Cambridge, MA 02139 USA. (e-mail: qsquek@mit.edu; moewin@mit.edu).

D. Dardari is with the WiLAB, DEIS & IEIIT/CNR, University of Bologna at Cesena, 47023 Cesena, Italy. (e-mail: ddardari@deis.unibo.it).

Digital Object Identifier 10.1109/TWC.2007.05748

[1] In order for this pair of separated signals to experience the same channel, either the time separation must be less than the channel coherence time, or the frequency separation must be less than the channel coherence bandwidth.

[45]. We then extend our BEP analysis to include NBI [50]. As in [23], we model NBI as a single-tone interferer with Rayleigh distributed amplitude.[2] We develop a quasi-analytical method as well as an approximate analytical method to evaluate the BEP of TR and DTR signaling in the presence of NBI. We show that the approximate analytical method is particularly useful in obtaining BEP expressions that provide insight into the effect of NBI. Numerical results reveal that the approximation agrees well with quasi-analytical results. We quantify the effects of NBI and channel power dispersion profile on the optimum integration interval of an AcR. We then compare TR and DTR signaling in terms of their sensitivity to NBI in both noise-limited and interference-limited regimes.

The paper is organized as follows. Section II presents the system and channel models for our signaling schemes. In Section III, a unified BEP analysis of TR and DTR signaling based on the sampling expansion approach is developed. The effect of NBI on the performance of TR and DTR signaling is studied in Section IV. To illustrate our proposed methodology, we consider Nakagami-m fading channels and present numerical examples in Section V. Finally, conclusions are given in the last section.

II. System and Channel Models

A. Transmitted-Reference

The transmitted signal of TR signaling for user k can be decomposed into a reference signal block $b_{\rm r}^{(k)}(t)$ and a data modulated signal block $b_{\rm d}^{(k)}(t)$ as given by

$$s_{\rm TR}^{(k)}(t) = \sum_i b_{\rm r}^{(k)}(t - iN_{\rm s}T_{\rm f}) + d_i^{(k)} b_{\rm d}^{(k)}(t - iN_{\rm s}T_{\rm f}), \quad (1)$$

where $T_{\rm f}$ is the average pulse repetition period, $d_i^{(k)} \in \{-1, 1\}$ is the ith data symbol, and $N_{\rm s}T_{\rm f}$ is the symbol duration [39]. The reference signal and modulated signal blocks, each consisting of $N_{\rm s}/2$ transmitted signal pulses, can be written as[3]

$$\begin{aligned} b_{\rm r}^{(k)}(t) &= \sum_{j=0}^{\frac{N_{\rm s}}{2}-1} \sqrt{E_{\rm p}} a_j^{(k)} p(t - j2T_{\rm f} - c_j^{(k)}T_{\rm p}), \\ b_{\rm d}^{(k)}(t) &= \sum_{j=0}^{\frac{N_{\rm s}}{2}-1} \sqrt{E_{\rm p}} a_j^{(k)} p(t - j2T_{\rm f} - c_j^{(k)}T_{\rm p} - T_{\rm r}), \quad (2) \end{aligned}$$

where $b_{\rm d}^{(k)}(t)$ is equal to a version of $b_{\rm r}^{(k)}(t)$, delayed by $T_{\rm r}$, and $p(t)$ is a unit energy bandpass signal pulse with duration $T_{\rm p}$ and center frequency $f_{\rm c}$. The energy of the transmitted pulse is then $E_{\rm p} = E_{\rm s}/N_{\rm s}$, where $E_{\rm s}$ is the symbol energy. In our case of binary signaling, the symbol energy equals the energy per bit, $E_{\rm b}$. To enhance the robustness of TR systems against interference and to allow multiple access, DS and/or TH spread spectrum techniques can be used as shown in (2). In DS signaling, $\{a_j^{(k)}\}$ is the bipolar pseudo-random sequence of the kth user.[4] In TH signaling, $\{c_j^{(k)}\}$ is the pseudo-random sequence of the kth user, where $c_j^{(k)}$ is an integer in the range $0 \le c_j^{(k)} < N_{\rm h}$, and $N_{\rm h}$ is the maximum allowable integer shift. A simplified example that illustrates TR signaling is shown in Fig. 1. The duration of the received UWB pulse is $T_{\rm g} = T_{\rm p} + T_{\rm d}$, where $T_{\rm d}$ is the maximum excess delay of the channel. To preclude inter-symbol interference (ISI) and intra-symbol interference (isi)[5], we assume that $T_{\rm r} \ge T_{\rm g}$ and $(N_{\rm h} - 1)T_{\rm p} + T_{\rm r} + T_{\rm g} \le 2T_{\rm f}$, where $T_{\rm r}$ is the time separation between each pair of data and reference pulses. If the symbol interval is less than the channel coherence time, all these pairs of separated signals will experience the same channel.[6] Note that $T_{\rm r}$ is constant for our case, as shown in Fig. 1, in contrast to [36], where the inter-pulse delays vary for different pairs of data-modulated and reference pulses.

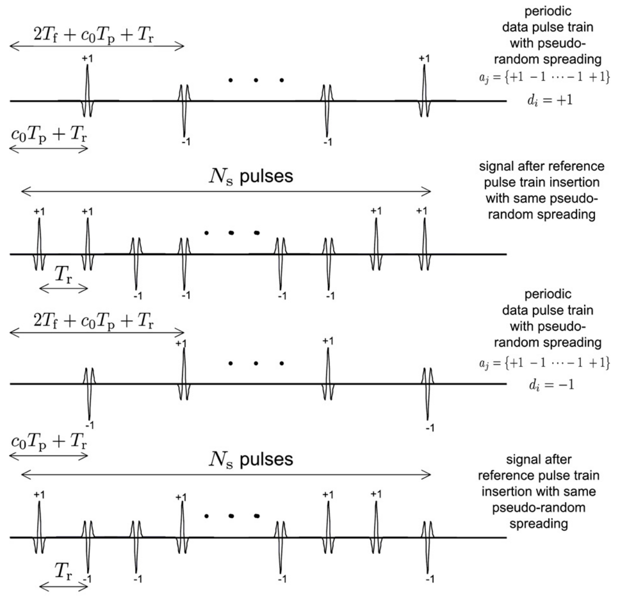

Fig. 1. Illustration of TR signaling scheme.

B. Differential Transmitted-Reference

The transmitted signal of DTR signaling for user k is given by

$$s_{\rm DTR}^{(k)}(t) = \sum_i e_i^{(k)} b^{(k)}(t - iN_{\rm s}T_{\rm f}), \quad (3)$$

where $b^{(k)}(t)$ is the kth user's block-modulated signal with symbol interval $N_{\rm s}T_{\rm f}$, and $N_{\rm s}$ is the number of transmitted signal pulses in each block. The data symbol $d_i^{(k)}$ is now differentially encoded such that $e_i^{(k)} = e_{i-1}^{(k)} d_i^{(k)}$, where $d_i^{(k)} \in \{-1, 1\}$. The $b^{(k)}(t)$-shaped signal block can be written as

$$b^{(k)}(t) = \sum_{j=0}^{N_{\rm s}-1} \sqrt{E_{\rm p}} a_j^{(k)} p(t - jT_{\rm f} - c_j^{(k)}T_{\rm p}), \quad (4)$$

[2]Results in [23] show that NBI can be reasonably well approximated by a tone interferer.

[3]Note that other combinations of data and reference pulses are also possible [51]. For simplicity and without loss of generality, we have adopted conventional TR signaling, in which the number of reference and data pulses are equal and $N_{\rm s}$ is even [37], [39], [46].

[4]Walsh-Hadamard sequences are used in [51].

[5]ISI and isi may not always be negligible due to constraints on $T_{\rm f}$ and data-rate requirements. In this case, our results will serve as a lower bound.

[6]For TR signaling with an AcR, only adjacent data and reference pulses need to be within the channel coherence time. The condition that all pulses within a symbol experience the same channel, however, will enable us to extend our analysis to TR signaling with a modified AcR, where the channel is assumed to be constant over two symbols.

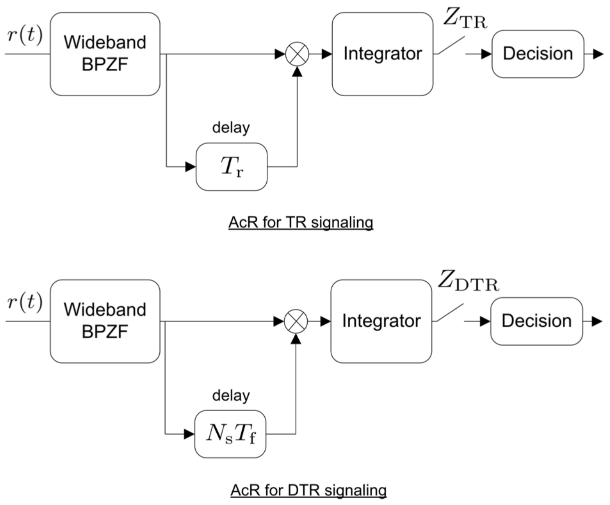

Fig. 2. AcR for TR and DTR signaling

where $\{a_j^{(k)}\}$ and $\{c_j^{(k)}\}$ are the DS and TH sequences that provide robustness to interference and multiple-access capability for DTR systems. Note that a DTR signal looks similar to a short-code CDMA signal, except that pulses are separated by at least $T_{\rm g}$ and TH is also present. The TH sequence is pseudo-random with the range $0 \leq c_j^{(k)} < N_{\rm h}$, where $N_{\rm h}$ satisfies $(N_{\rm h}-1)T_{\rm p}+T_{\rm g} \leq T_{\rm f}$ to preclude ISI and isi. The channel must be constant over two symbols in order to use differential encoding over two adjacent symbols.

C. Channel model

The received signal for TR signaling can be written as $r(t) = (h * s_{\rm TR})(t) + n(t)$, where $h(t)$ is the impulse response of the channel and $n(t)$ is zero-mean, white Gaussian noise with two-sided power spectral density $N_0/2$. Note that a similar equation also applies to DTR signaling by replacing $s_{\rm TR}(t)$ with $s_{\rm DTR}(t)$. The channel impulse response, modeled as linear time-invariant, can be written as $h(t) = \sum_{l=1}^{L} \alpha_l \delta(t-\tau_l)$, where L is the number of resolvable multipath components, and α_l and τ_l respectively denote the attenuation and delay of lth path. We can express $\alpha_l = |\alpha_l| \exp(j\phi_l)$, where $\phi_l = 0$ or π with equal probability. As in [7], [8], we consider the resolvable dense multipath channel,[7] i.e., $|\tau_l - \tau_j| \geq T_{\rm p}, \forall l \neq j$, where $\tau_l = \tau_1 + (l-1)T_{\rm p}$, and $\{\alpha_l\}$ are assumed to be statistically independent random variables (r.v.'s).

III. Receiver Models

This paper focuses on a single user system. As a result, we will suppress the index k for notational simplicity in the rest of the paper. We assume perfect synchronization at the receiver.[8]

[7]Such an assumption may not be always true [52], [53]. However, the dense resolvable multipath channel serves as a reasonable approximation to realistic UWB channels. Therefore, our BEP analysis still provides insight into the performance of TR signaling.

[8]It has been shown that we can relax the assumption of perfect synchronization in TR signaling due to its robustness against synchronization errors [54], [55]. However, exactly how this synchronization is achieved [54], [56] and the sensitivity analysis of synchronization errors [55] are beyond the scope of this paper.

Without loss of generality, we consider the detection of the data symbol at $i = 0$.

A. Autocorrelation Receiver

As shown in Fig. 2, the AcR first passes the received signal through an ideal bandpass zonal filter (BPZF) with center frequency $f_{\rm c}$ to eliminate out-of-band noise. If the bandwidth W of the BPZF is large enough, then the signal spectrum will pass through undistorted. Consequently, the ISI and isi caused by filtering will be negligible. In this case, the output of the BPZF for TR and DTR signaling can be expressed respectively as

$$\begin{aligned}\widetilde{r}_{\rm TR}(t) &= \sum_i \sum_{j=0}^{\frac{N_{\rm s}}{2}-1} \sum_{l=1}^{L} \Big[\sqrt{E_{\rm p}}\alpha_l a_j p(t - iN_{\rm s}T_{\rm f} - j2T_{\rm f} - c_jT_{\rm p} - \tau_l) \\ &\quad + \sqrt{E_{\rm p}}\alpha_l a_j d_i p(t - iN_{\rm s}T_{\rm f} - j2T_{\rm f} - c_jT_{\rm p} - T_{\rm r} - \tau_l)\Big] \\ &\quad + \widetilde{n}(t), \end{aligned} \tag{5}$$

and

$$\begin{aligned}\widetilde{r}_{\rm DTR}(t) &= \sum_i \sum_{j=0}^{N_{\rm s}-1} \sum_{l=1}^{L} \sqrt{E_{\rm p}}\alpha_l a_j e_i p(t - iN_{\rm s}T_{\rm f} - jT_{\rm f} - c_jT_{\rm p} - \tau_l) \\ &\quad + \widetilde{n}(t), \end{aligned} \tag{6}$$

where $\widetilde{n}(t)$ is a zero-mean, Gaussian random process with autocorrelation function

$$R_{\widetilde{n}}(\tau) = WN_0 \,\mathrm{sinc}(W\tau)\cos(2\pi f_{\rm c}\tau). \tag{7}$$

Note that when $W \gg 1/T_{\rm g}$, $R_{\widetilde{n}}(\tau)$ in (7) is approximately equal to zero for $|\tau| \geq T_{\rm g}$. This implies that the noise samples separated by more than $T_{\rm g}$ or at a multiple of $1/W$ are statistically independent.

The filtered received signal is passed through a correlator with integration interval T ($T_{\rm p} \leq T \leq T_{\rm g}$), as shown in Fig. 2, to collect the received signal energy. The integration interval T determines the number of multipath components (or equivalently, the amount of energy) captured by the receiver, as well as the amount of noise and interference accumulation. As will be shown in later sections, the optimum T depends on various channel conditions, such as the decay factor of the channel power dispersion profile (PDP), and on the signal-to-interference ratios (SIR's). The decision statistics generated at the integrator output of the AcR can be written respectively as

$$Z_{\rm TR} = \sum_{j=0}^{\frac{N_{\rm s}}{2}-1} \int_{j2T_{\rm f}+T_{\rm r}+c_jT_{\rm p}}^{j2T_{\rm f}+T_{\rm r}+c_jT_{\rm p}+T} \widetilde{r}_{\rm TR}(t)\,\widetilde{r}_{\rm TR}(t-T_{\rm r})dt, \tag{8}$$

and

$$Z_{\rm DTR} = \sum_{j=0}^{N_{\rm s}-1} \int_{jT_{\rm f}+c_jT_{\rm p}}^{jT_{\rm f}+c_jT_{\rm p}+T} \widetilde{r}_{\rm DTR}(t)\,\widetilde{r}_{\rm DTR}(t-N_{\rm s}T_{\rm f})dt, \tag{9}$$

for TR and DTR signaling.

$$Z_{\rm ATR} = \sum_{j=0}^{\frac{N_{\rm s}}{2}-1} a_j \int_{j2T_{\rm f}+T_{\rm r}+c_jT_{\rm p}}^{j2T_{\rm f}+T_{\rm r}+c_jT_{\rm p}+T} \widetilde{r}_{\rm TR}(t) \left[\frac{2}{N_{\rm s}} \sum_{k=-j}^{\frac{N_{\rm s}}{2}-1-j} a_{j+k}\widetilde{r}_{\rm TR}\Big(t-(N_{\rm s}-2k)T_{\rm f}-(c_j-c_{j+k})T_{\rm p}-T_{\rm r}\Big)\right] dt, \quad (10)$$

$$Z_{\rm ADTR} = \sum_{j=0}^{N_{\rm s}-1} a_j \int_{jT_{\rm f}+c_jT_{\rm p}}^{jT_{\rm f}+c_jT_{\rm p}+T} \widetilde{r}_{\rm DTR}(t) \left[\frac{1}{N_{\rm s}} \sum_{k=-j}^{N_{\rm s}-1-j} a_{j+k}\widetilde{r}_{\rm DTR}\Big(t-(N_{\rm s}-k)T_{\rm f}-(c_j-c_{j+k})T_{\rm p}\Big)\right] dt. \quad (11)$$

B. Modified Autocorrelation Receiver

The AcR performance for both TR and DTR signaling can be improved by averaging respectively over $N_{\rm s}/2$ and $N_{\rm s}$ received reference pulses from the previous symbol [37]–[39], [45].[9] This, however, requires the channel to remain constant over two symbols. The decision statistics of this modified AcR for TR and DTR signaling are given respectively by (10) and (11), shown at the top of this page. Next, we develop an analytical framework based on the sampling expansion approach to provide a unified performance analysis of TR and DTR systems in dense multipath channels.

IV. Performance Analysis

A. Transmitted-Reference

We begin by deriving the BEP for TR signaling with an AcR in the absence of NBI. It can be shown that $Z_{\rm TR}$ in (8) can be written as [38], [39]

$$\begin{aligned} Z_{\rm TR} &= \sum_{j=0}^{\frac{N_{\rm s}}{2}-1} \int_0^T \Big[\breve{b}_{\rm r}(t+j2T_{\rm f}+c_jT_{\rm p}) + \widetilde{n}(t+j2T_{\rm f}+c_jT_{\rm p})\Big] \\ &\quad \times \Big[d_0\breve{b}_{\rm d}(t+j2T_{\rm f}+c_jT_{\rm p}+T_{\rm r}) \\ &\qquad + \widetilde{n}(t+j2T_{\rm f}+c_jT_{\rm p}+T_{\rm r})\Big] dt, \end{aligned} \quad (12)$$

where $\breve{b}_{\rm r}(t) \triangleq (b_{\rm r} * h * h_{\rm ZF})(t)$, $\breve{b}_{\rm d}(t) \triangleq (b_{\rm d} * h * h_{\rm ZF})(t)$, and $h_{\rm ZF}(t)$ is the impulse response of the BPZF. Note that if the symbol interval is less than the coherence time, all pairs of separated pulses will experience the same channel; hence $\breve{b}_{\rm r}(t+j2T_{\rm f}+c_jT_{\rm p}) = \breve{b}_{\rm d}(t+j2T_{\rm f}+c_jT_{\rm p}+T_{\rm r})$ for all $t \in (0,T)$ and j. In this case, we can significantly simplify the expression in (12) as follows:

$$\begin{aligned} Z_{\rm TR} &= \sum_{j=0}^{\frac{N_{\rm s}}{2}-1} \int_0^T \Big[w_j(t)+\eta_{1,j}(t)\Big]\Big[d_0 w_j(t)+\eta_{2,j}(t)\Big] dt \\ &= \sum_{j=0}^{\frac{N_{\rm s}}{2}-1} U_j, \end{aligned} \quad (13)$$

where we have used $w_j(t) \triangleq \breve{b}_{\rm r}(t+j2T_{\rm f}+c_jT_{\rm p}) = \sqrt{E_{\rm p}}a_j\sum_{l=1}^{L}\alpha_l p(t-\tau_l)$, $\eta_{1,j}(t) \triangleq \widetilde{n}(t+j2T_{\rm f}+c_jT_{\rm p})$, and $\eta_{2,j}(t) \triangleq \widetilde{n}(t+j2T_{\rm f}+c_jT_{\rm p}+T_{\rm r})$, all defined over the interval $[0,T]$. Note that because the noise samples are taken at least $T_{\rm g}$ apart, they are essentially independent, regardless of c_j.[10] We further observe that U_j is simply the integrator output corresponding to the jth received modulated monocycle. Following the sampling expansion approach in [38], [39], we can represent U_j as

$$\begin{aligned} U_j = \frac{1}{2W}\sum_{m=1}^{2WT} \big(&d_0 w_{j,m}^2 + w_{j,m}\eta_{2,j,m} \\ &+ d_0 w_{j,m}\eta_{1,j,m} + \eta_{1,j,m}\eta_{2,j,m}\big), \end{aligned} \quad (14)$$

where $w_{j,m}$, $\eta_{1,j,m}$, and $\eta_{2,j,m}$, for odd m (even m) are the real (imaginary) parts of the samples of the equivalent low-pass version of $w_j(t)$, $\eta_{1,j}(t)$, and $\eta_{2,j}(t)$, respectively, sampled at Nyquist rate W over the interval $[0,T]$.

Conditioned on d_0 and $a_j = +1$, we can express (14) in the form of a summation of squares:

$$U_{j|d_0=+1} = \sum_{m=1}^{2WT}\left[\left(\frac{1}{\sqrt{2W}}w_{j,m}+\beta_{1,j,m}\right)^2 - \beta_{2,j,m}^2\right], \quad (15)$$

$$U_{j|d_0=-1} = \sum_{m=1}^{2WT}\left[-\left(\frac{1}{\sqrt{2W}}w_{j,m}-\beta_{2,j,m}\right)^2 + \beta_{1,j,m}^2\right], \quad (16)$$

where $\beta_{1,j,m} = \frac{1}{2\sqrt{2W}}(\eta_{2,j,m}+\eta_{1,j,m})$ and $\beta_{2,j,m} = \frac{1}{2\sqrt{2W}}(\eta_{2,j,m}-\eta_{1,j,m})$ are statistically independent Gaussian r.v.'s with variance $\sigma_{\rm TR}^2 = \frac{N_0}{4}$. Due to the statistical symmetry of U_j with respect to d_0 and $\{a_j\}$, we simply need to calculate the BEP conditioned on $d_0 = +1$ and $a_j = +1$. For notational simplicity, we define the normalized r.v.'s Y_1, Y_2, Y_3, and Y_4 as

$$\begin{aligned} Y_1 &\triangleq \frac{1}{2\sigma_{\rm TR}^2}\sum_{j=0}^{\frac{N_{\rm s}}{2}-1}\sum_{m=1}^{2WT}\left(\frac{1}{\sqrt{2W}}w_{j,m}+\beta_{1,j,m}\right)^2, \\ Y_2 &\triangleq \frac{1}{2\sigma_{\rm TR}^2}\sum_{j=0}^{\frac{N_{\rm s}}{2}-1}\sum_{m=1}^{2WT}\beta_{2,j,m}^2, \\ Y_3 &\triangleq \frac{1}{2\sigma_{\rm TR}^2}\sum_{j=0}^{\frac{N_{\rm s}}{2}-1}\sum_{m=1}^{2WT}\left(\frac{1}{\sqrt{2W}}w_{j,m}-\beta_{2,j,m}\right)^2, \\ Y_4 &\triangleq \frac{1}{2\sigma_{\rm TR}^2}\sum_{j=0}^{\frac{N_{\rm s}}{2}-1}\sum_{m=1}^{2WT}\beta_{1,j,m}^2. \end{aligned} \quad (17)$$

Conditioned on the channel, Y_1 and Y_3 are noncentral chi-squared r.v.'s, whereas Y_2 and Y_4 are central chi-squared r.v.'s each having $N_{\rm s}WT$ degrees of freedom. Both Y_1 and Y_3 have

[9] This averaging can be thought of as forming an estimate of the channel. In fact, when the observation noise is Gaussian, this is equivalent to forming a maximum likelihood estimate of the channel [57].

[10] As a result, no assumption on c_j is required since the above analysis is independent of $\{c_j\}$.

TABLE I
TR SIGNALING SCHEMES

Signaling	Non-centrality parameter of Y_1	Variance of $\beta_{1,j,m}$	Degrees of freedom of Y_1
TR	$\frac{E_s}{N_0}\sum_{l=1}^{L_{CAP}}\alpha_l^2$	$\frac{N_0}{4}$	$\frac{N_sWT}{2}$
ATR	$\frac{2N_s}{(N_s+2)}\left(\frac{E_s}{N_0}\sum_{l=1}^{L_{CAP}}\alpha_l^2\right)$	$\frac{N_0(N_s+2)}{8N_s}$	$\frac{N_sWT}{2}$
DTR	$\frac{2E_s}{N_0}\sum_{l=1}^{L_{CAP}}\alpha_l^2$	$\frac{N_0}{4}$	N_sWT
ADTR	$\frac{4N_s}{(N_s+1)}\left(\frac{E_s}{N_0}\sum_{l=1}^{L_{CAP}}\alpha_l^2\right)$	$\frac{N_0(N_s+1)}{8N_s}$	N_sWT

the same non-centrality parameter, given by

$$\mu_{\mathrm{TR}} = \frac{1}{2\sigma_{\mathrm{TR}}^2}\sum_{j=0}^{\frac{N_s}{2}-1}\int_0^T w_j^2(t)dt = \frac{E_s}{N_0}\sum_{l=1}^{L_{\mathrm{CAP}}}\alpha_l^2, \tag{18}$$

where $L_{\mathrm{CAP}} \triangleq \lceil \min\{WT, WT_g\}\rceil$ denotes the actual number of multipath components captured by the AcR. The probability density functions (pdfs) of Y_1 and Y_2 conditioned on μ_{TR} are given by

$$f_{Y_1|\mu_{\mathrm{TR}}}(y_1) = f_{\mathrm{NC}}(y_1, \mu_{\mathrm{TR}}, q_{\mathrm{TR}}), \tag{19}$$
$$f_{Y_2|\mu_{\mathrm{TR}}}(y_2) = f_{\mathrm{C}}(y_2, q_{\mathrm{TR}}), \tag{20}$$

where $q_{\mathrm{TR}} = \frac{N_sWT}{2}$. We have defined the following pdfs for notational convenience

$$f_{\mathrm{NC}}(y,\mu,n) \triangleq e^{-(y+\mu)}\left(\frac{y}{\mu}\right)^{\frac{(n-1)}{2}} I_{n-1}\left(2\sqrt{y\mu}\right), \quad y \geq 0$$
$$f_{\mathrm{C}}(y,n) \triangleq \frac{y^{(n-1)}}{(n-1)!}\exp(-y), \quad y \geq 0$$

where $I_{n-1}(\cdot)$ is the $(n-1)$th order modified Bessel function of the first kind. The functions $f_{\mathrm{NC}}(y,\mu,n)$ and $f_{\mathrm{C}}(y,n)$ respectively are the pdfs of the noncentral and central chi-squared r.v.'s with $2n$ degrees of freedom and non-centrality parameter μ [58]. Using (19) and (20), the BEP of TR signaling with an AcR is given by

$$\begin{aligned}P_{e,\mathrm{TR}} &= \mathbb{P}\{Z_{\mathrm{TR}} \leq 0 | d_0 = +1\} \\ &= \mathbb{E}_{\mu_{\mathrm{TR}}}\{\mathbb{P}\{Y_1 < Y_2 | d_0 = +1\}\} \\ &= \frac{1}{2^{q_{\mathrm{TR}}}}\left[\sum_{n=0}^{q_{\mathrm{TR}}-1}\left(\frac{(-j)^n}{n!}\right)\frac{d^n}{dv^n}\psi_{\mu_{\mathrm{TR}}}(jv/2)\bigg|_{jv=-1} \right.\\ &\quad \left.\times\sum_{k=n}^{q_{\mathrm{TR}}-1}\frac{1}{2^k}\frac{(k+q_{\mathrm{TR}}-1)!}{(k-n)!(q_{\mathrm{TR}}+n-1)!}\right] \\ &\triangleq P_e(\psi_{\mu_{\mathrm{TR}}}(jv), q_{\mathrm{TR}}),\end{aligned} \tag{21}$$

where $\psi_{\mu_{\mathrm{TR}}}(jv) \triangleq \mathbb{E}\{\exp(jv\mu_{\mathrm{TR}})\}$ is the characteristic function (CF) of μ_{TR}. When the channel is resolvable and multipath components are statistically independent, $\psi_{\mu_{\mathrm{TR}}}(jv) = \prod_{l=1}^{L_{\mathrm{CAP}}}\psi_l(\frac{jvE_s}{N_0})$, where $\psi_l(jv)$ is the CF of α_l^2 whose closed-form expression is known for a broad class of channel fading statistics [58]. The detailed derivation of (21) can be found in [38], [39], [45].

Next, we extend the above analysis to derive the BEP of TR signaling with a modified AcR [38], [39], [45]. In this case, the non-centrality parameter of Y_1 in (17) becomes

$$\mu_{\mathrm{ATR}} \triangleq \frac{1}{2\sigma_{\mathrm{ATR}}^2}\sum_{j=0}^{\frac{N_s}{2}-1}\int_0^T w_j^2(t)dt = \frac{2N_s}{N_s+2}\left(\frac{E_s}{N_0}\sum_{l=1}^{L_{\mathrm{CAP}}}\alpha_l^2\right). \tag{22}$$

As shown in Table I, the non-centrality parameter of a modified AcR (eq. (22)) is at most two times larger than that of AcR (eq. (18)). Using (21), the BEP of TR signaling with a modified AcR can be written as

$$P_{e,\mathrm{ATR}} = P_e(\psi_{\mu_{\mathrm{ATR}}}(jv), q_{\mathrm{TR}}). \tag{23}$$

B. Differential Transmitted-Reference

We begin by deriving the BEP for DTR signaling with an AcR in the absence of NBI, following an approach similar to the case of TR signaling. In this case, we can represent U_j as

$$U_j = \frac{1}{2W}\sum_{m=1}^{2WT}\left(d_0 w_{j,m}^2 + e_{-1}w_{j,m}\eta_{2,j,m} + e_0 w_{j,m}\eta_{1,j,m} + \eta_{1,j,m}\eta_{2,j,m}\right), \tag{24}$$

where $w_{j,m}$, $\eta_{1,j,m}$, and $\eta_{2,j,m}$, for odd m (even m) are the real (imaginary) parts of the samples of the equivalent low-pass version of $w_j(t) \triangleq (b * h * h_{\mathrm{ZF}})(t + jT_f + c_jT_p) = \sqrt{E_p}a_j\sum_{l=1}^{L}\alpha_l p(t-\tau_l)$, $\eta_{1,j}(t) \triangleq \widetilde{n}(t+jT_f+c_jT_p-N_sT_f)$, and $\eta_{2,j}(t) \triangleq \widetilde{n}(t+jT_f+c_jT_p)$, respectively, sampled at Nyquist rate W over the interval $[0,T]$.

Similar to TR signaling, our following analysis requires no assumption on $\{c_j\}$, and we exploit statistical symmetry of U_j with respect to d_0 and $\{a_j\}$. Conditioned on $d_0 = +1$, we can express (24) in the form of (15),[11] where in this case $\beta_{1,j,m} = \frac{1}{2\sqrt{2W}}(e_{-1}\eta_{2,j,m} + e_0\eta_{1,j,m})$ and $\beta_{2,j,m} = \frac{1}{2\sqrt{2W}}(e_{-1}\eta_{2,j,m} - e_0\eta_{1,j,m})$ are statistically independent Gaussian r.v.'s. with variance $\sigma_{\mathrm{DTR}}^2 = \frac{N_0}{4}$. Due to symmetry, we only need to

[11]When $d_0 = +1$, the pairs of differentially encoded bits are either $(e_{-1}, e_0) = (+1,+1)$ or $(e_{-1}, e_0) = (-1,-1)$ with probability $\frac{1}{2}$ each. By symmetry, we only need to consider $(e_{-1}, e_0) = (+1,+1)$.

consider Y_1 and Y_2 in (17), where the non-centrality parameter of Y_1 is now given by

$$\mu_{\rm DTR} \triangleq \frac{1}{2\sigma^2_{\rm DTR}} \sum_{j=0}^{N_{\rm s}-1} \int_0^T w_j^2(t)dt = \frac{2E_{\rm s}}{N_0} \sum_{l=1}^{L_{\rm CAP}} \alpha_l^2, \quad (25)$$

and the pdfs of Y_1 and Y_2 conditioned on $\mu_{\rm DTR}$ are given by

$$f_{Y_1|\mu_{\rm DTR}}(y_1) = f_{\rm NC}(y_1, \mu_{\rm DTR}, q_{\rm DTR}), \quad (26)$$
$$f_{Y_2|\mu_{\rm DTR}}(y_2) = f_{\rm C}(y_2, q_{\rm DTR}), \quad (27)$$

where $q_{\rm DTR} = N_{\rm s}WT$. As shown in Table I, we can observe that the basic difference between TR and DTR signaling lies not only in a doubled non-centrality parameter, but also in double the degrees of freedom. The non-centrality parameter reflects the amount of useful energy captured by the correlator at the receiver, hence, larger values result in better performance. On the contrary, the degrees of freedom of Y_1 account for the noise accumulation in the integration interval; thus, larger values result in poorer performance. Following the derivation leading to (21), the BEP of DTR signaling with an AcR can be written as

$$P_{\rm e,DTR} = P_{\rm e}(\psi_{\mu_{\rm DTR}}(jv), q_{\rm DTR}), \quad (28)$$

where $\psi_{\mu_{\rm DTR}}(jv) \triangleq \mathbb{E}\{\exp(jv\mu_{\rm DTR})\} = \prod_{l=1}^{L_{\rm CAP}} \psi_l(\frac{jv2E_{\rm s}}{N_0})$ is the CF of $\mu_{\rm DTR}$.

For DTR signaling with a modified AcR, the non-centrality parameter of Y_1 in (17) becomes

$$\mu_{\rm ADTR} \triangleq \frac{1}{2\sigma^2_{\rm ADTR}} \sum_{j=0}^{N_{\rm s}-1} \int_0^T w_j^2(t)dt = \frac{4N_{\rm s}}{(N_{\rm s}+1)} \left(\frac{E_{\rm s}}{N_0} \sum_{l=1}^{L_{\rm CAP}} \alpha_l^2\right), \quad (29)$$

where the variance $\sigma^2_{\rm ADTR}$ of $\beta_{1,j,m}$ and $\beta_{2,j,m}$ is[12]

$$\sigma^2_{\rm ADTR} = \frac{\mathbb{V}\{e_{i-1}\eta_{2,j,m}\} + \mathbb{V}\{e_i\eta_{1,j,m}\}}{8W} = \frac{N_0(N_{\rm s}+1)}{8N_{\rm s}}. \quad (30)$$

The pdfs of Y_1 and Y_2 conditioned on $\mu_{\rm ADTR}$ are now given by

$$f_{Y_1|\mu_{\rm ADTR}}(y_1) = f_{\rm NC}(y_1, \mu_{\rm ADTR}, q_{\rm DTR}), \quad (31)$$
$$f_{Y_2|\mu_{\rm ADTR}}(y_2) = f_{\rm C}(y_2, q_{\rm DTR}). \quad (32)$$

Following the derivation leading to (21), the BEP of DTR signaling with a modified AcR is given by

$$P_{\rm e,ADTR} = P_{\rm e}(\psi_{\mu_{\rm ADTR}}(jv), q_{\rm DTR}). \quad (33)$$

In the next section, we extend our BEP analysis of TR and DTR signaling to include NBI.

V. Narrowband Interference Analysis

In the presence of NBI, the received signal can be written as $r(t) = (h * s)(t) + J(t) + n(t)$, where $J(t)$ denotes the NBI and $s(t)$ denotes the signal transmitted via TR or DTR signaling. The autocorrelation function of the superposition of the two independent noise processes, $n_{\rm T}(t) \triangleq J(t) + n(t)$, is given by $R_{n_{\rm T}}(\tau) = R_{\rm J}(\tau) + \frac{N_0}{2}\delta(\tau)$, where $R_{\rm J}(\tau) = \mathbb{E}\{J(t)J(t+\tau)\}$. Since the bandwidth of typical NBI is smaller than that of the transmitted pulse, the autocorrelation function of $\widetilde{n}_{\rm T}(t)$, the bandpass filtered version of $n_{\rm T}(t)$, is given by

$$R_{\widetilde{n}_{\rm T}}(\tau) = R_{\rm J}(\tau) + WN_0 \,\mathrm{sinc}(W\tau)\cos(2\pi f_{\rm c}\tau). \quad (34)$$

As in [23], we model the NBI as a single-tone continuous-wave signal given by

$$J(t) = \alpha_{\rm J}\sqrt{2J_0}\cos(2\pi f_{\rm J} t + \theta), \quad (35)$$

where J_0 is the average NBI power, $\alpha_{\rm J}$ is a slowly-varying Rayleigh distributed r.v. with $\mathbb{E}\{\alpha_{\rm J}^2\} = 1$, $f_{\rm J}$ is the NBI carrier frequency, and θ is the random phase, uniformly distributed over $[0, 2\pi)$.[13] Thus, $R_{\rm J}(\tau) = J_0\cos(2\pi f_{\rm J}\tau)$, which means that $\widetilde{n}_{\rm T}(t)$ is colored, and the samples of $\widetilde{n}_{\rm T}(t)$ taken at an interval of $1/W$ are correlated. In the following, we derive the BEP of TR and DTR signaling with an AcR in the presence of NBI, where we define $\mathsf{SIR} \triangleq E_{\rm s}/(N_{\rm s}T_{\rm f}J_0)$. The extension to modified AcR is straightforward and omitted for brevity.

A. Transmitted-Reference

By incorporating the NBI given in (35) and using the sampling expansion approach, we can rewrite U_j in (14) as

$$U_j = \frac{1}{2W}\sum_{m=1}^{2WT}\Big[d_0 w_{j,m}^2 + w_{j,m}(\xi_{2,j,m} + \eta_{2,j,m}) + d_0 w_{j,m}(\xi_{1,j,m} + \eta_{1,j,m}) + (\xi_{1,j,m} + \eta_{1,j,m})(\xi_{2,j,m} + \eta_{2,j,m})\Big], \quad (36)$$

where $\xi_{1,j,m}$ and $\xi_{2,j,m}$, for odd m (even m) respectively are the real (imaginary) parts of the samples of the equivalent low-pass version of $\xi_{1,j}(t)$ and $\xi_{2,j}(t)$, given by

$$\xi_{1,j}(t) = \alpha_{\rm J}\sqrt{2J_0}\cos\left[2\pi f_{\rm J}\left(t + j2T_{\rm f} + c_jT_{\rm p}\right) + \theta\right],$$
$$\xi_{2,j}(t) = \alpha_{\rm J}\sqrt{2J_0}\cos\left[2\pi f_{\rm J}\left(t + j2T_{\rm f} + c_jT_{\rm p} + T_{\rm r}\right) + \theta\right]. \quad (37)$$

The rest of the terms in (36) are defined similarly to those in (14). By conditioning on d_0, we can rewrite (36) in the form of (15) and (16), where $\beta_{1,j,m} = \frac{1}{2\sqrt{2W}}(\eta_{2,j,m} + \xi_{2,j,m} + \eta_{1,j,m} + \xi_{1,j,m})$ and $\beta_{2,j,m} = \frac{1}{2\sqrt{2W}}(\eta_{2,j,m} + \xi_{2,j,m} - \eta_{1,j,m} - \xi_{1,j,m})$. Further conditioning on θ, $\alpha_{\rm J}$, and $\{c_j\}$, the quantities $\xi_{1,j,m}$ and $\xi_{2,j,m}$ in (37) are deterministic, and the conditional variance $\sigma^2_{\rm TR}$ of $\beta_{1,j,m}$ and $\beta_{2,j,m}$ is simply $\frac{N_0}{4}$. Thus, the statistical characterization of U_j when conditioned on θ, $\alpha_{\rm J}$, $\{c_j\}$, $\{a_j\}$, and $\{\alpha_l\}$ is no longer symmetric with respect to d_0 due to the presence of the interference term. Note that $U_{j|d_0=+1}$ is simply the difference of two noncentral chi-squared r.v.'s with the same degrees of freedom, but different non-centrality parameters. As a result, we need to separately calculate the conditional BEP with respect to d_0 to obtain the overall BEP.

[12]The notation $\mathbb{V}\{x\}$ denotes the variance of r.v. x.

[13]Unlike UWB signals, NBI experiences frequency flat fading and the amplitude $\alpha_{\rm J}$ is assumed to be constant over at least two symbols of TR signaling.

$$\begin{aligned}\mu_{\mathrm{TR},Y_1}^{(\mathrm{NBI})} &\triangleq \frac{1}{2\sigma_{\mathrm{TR}}^2}\sum_{j=0}^{\frac{N_\mathrm{s}}{2}-1}\int_0^T\left[w_j(t)+\frac{\xi_{1,j}(t)+\xi_{2,j}(t)}{2}\right]^2 dt\\ &\approx \frac{E_\mathrm{s}}{N_0}\sum_{l=1}^{L_\mathrm{CAP}}\alpha_l^2+\frac{\alpha_\mathrm{J}^2 N_\mathrm{s} J_0 T}{2N_0}+\frac{\alpha_\mathrm{J}^2 N_\mathrm{s} J_0 T}{2N_0}\cos(2\pi f_\mathrm{J} T_\mathrm{r})\\ &\quad+\frac{4\alpha_\mathrm{J}|\widehat{P}(f_\mathrm{J})|\sqrt{2E_\mathrm{p}J_0}\cos(\pi f_\mathrm{J} T_\mathrm{r})}{N_0}\sum_{j=0}^{\frac{N_\mathrm{s}}{2}-1}a_j\sum_{l=1}^{L_\mathrm{CAP}}\alpha_l\cos\left(2\pi f_\mathrm{J}\left(\tau_l+j2T_\mathrm{f}+c_jT_\mathrm{p}+T_\mathrm{r}/2\right)+\varphi\right),\end{aligned}\tag{38}$$

$$\mathbb{P}\{Z_\mathrm{TR}\le 0|d_0=+1\}=\frac{1}{2}+\frac{1}{\pi}\int_0^\infty\left(\frac{1}{1+v^2}\right)^{q_\mathrm{TR}}\mathfrak{Re}\left\{\frac{\mathbb{E}_\Psi\left\{\exp\left(\frac{-jv\mu_{\mathrm{TR},Y_1}^{(\mathrm{NBI})}}{1+jv}\right)\exp\left(\frac{jv\mu_{\mathrm{TR},Y_2}^{(\mathrm{NBI})}}{1-jv}\right)\right\}}{jv}\right\}dv,\tag{42}$$

$$\begin{aligned}\mathbb{P}\{Z_\mathrm{TR}\le 0|d_0=+1\}&\simeq\frac{1}{2}+\frac{1}{\pi}\int_0^\infty\left(\frac{1}{1+v^2}\right)^{q_\mathrm{TR}}\mathfrak{Re}\left\{\frac{\mathbb{E}_{\{\alpha_l\},\alpha_\mathrm{J}}\left\{\exp\left(\frac{-jv\mu_{\mathrm{TR},Y_1}^{(\mathrm{NBI})}}{1+jv}\right)\exp\left(\frac{jv\mu_{\mathrm{TR},Y_2}^{(\mathrm{NBI})}}{1-jv}\right)\right\}}{jv}\right\}dv\\ &=\frac{1}{2}+\frac{1}{\pi}\int_0^\infty\left(\frac{1}{1+v^2}\right)^{q_\mathrm{TR}}\mathfrak{Re}\left\{\frac{\psi_{\mu_\mathrm{TR}}\left(\frac{-jv}{1+jv}\right)\psi_\mathrm{J}\left(g_{\mathrm{TR},d_0=+1}(jv)\right)}{jv}\right\}dv\\ &\triangleq P_\mathrm{e}^{(\mathrm{NBI})}\Big(\psi_{\mu_\mathrm{TR}}(jv),\psi_\mathrm{J}\left(g_{\mathrm{TR},d_0=+1}(jv)\right),q_\mathrm{TR}\Big),\end{aligned}\tag{43}$$

First, we derive the non-centrality parameters of Y_1 and Y_2 when conditioned on Ψ in (38) (at the top of this page) and (39), respectively:

$$\begin{aligned}\mu_{\mathrm{TR},Y_2}^{(\mathrm{NBI})}&\triangleq\frac{1}{8\sigma_\mathrm{TR}^2}\sum_{j=0}^{\frac{N_\mathrm{s}}{2}-1}\int_0^T(\xi_{2,j}(t)-\xi_{1,j}(t))^2dt\\ &\approx\frac{\alpha_\mathrm{J}^2N_\mathrm{s}J_0T}{2N_0}-\frac{\alpha_\mathrm{J}^2N_\mathrm{s}J_0T}{2N_0}\cos(2\pi f_\mathrm{J}T_\mathrm{r}),\end{aligned}\tag{39}$$

where Ψ is defined for notational convenience as $\Psi \triangleq \left\{\alpha_\mathrm{J},\{\alpha_l\}_{l=1}^{L},\varphi,\{c_j\}_{j=1}^{N_\mathrm{s}/2},\{a_j\}_{j=1}^{N_\mathrm{s}/2}\right\}$. The detailed derivation and the justification of the approximations leading to (38) and (39), as well as the definition of φ and $\widehat{P}(f_\mathrm{J})$ can be found in Appendix I. Note that Y_2 in (17) is now a noncentral chi-squared r.v. due to the presence of NBI. From (38) and (39), it is interesting to see that the NBI affects the performance by changing the conditional means and variances of Y_1 and Y_2.[14] Using (38) and (39), the conditional pdfs of Y_1 and Y_2 are given by

$$f_{Y_1|\Psi}(y_1)=f_\mathrm{NC}\left(y_1,\mu_{\mathrm{TR},Y_1}^{(\mathrm{NBI})},q_\mathrm{TR}\right),\tag{40}$$

$$f_{Y_2|\alpha_\mathrm{J}}(y_2)=f_\mathrm{NC}\left(y_2,\mu_{\mathrm{TR},Y_2}^{(\mathrm{NBI})},q_\mathrm{TR}\right),\tag{41}$$

where we have suppressed the conditioning r.v.'s $\{\alpha_l\}$, φ, $\{c_j\}$, and $\{a_j\}$ in (41) since (39) does not depend on these r.v.'s. Now, to evaluate the BEP for $Z_\mathrm{TR}\le 0$ when $d_0=+1$, we use the inversion theorem [59] to obtain (42), shown at the top of this page, where $\mathfrak{Re}\{\cdot\}$ denotes the real part. By resorting to a quasi-analytical method, the statistical expectation in (42) can be calculated by numerically averaging each argument within the expectation with respect to its corresponding r.v.'s. Alternatively, we can resort to an approximate analytical method, where we consider the last term in (38) negligible compared to the first two terms. As a result, we can further suppress the conditioning r.v.'s φ, $\{c_j\}$, and $\{a_j\}$ in (40), since the dependence of $\mu_{\mathrm{TR},Y_1}^{(\mathrm{NBI})}$ on these r.v.'s is now negligible. The approximate BEP conditioned on $d_0=+1$ can be rewritten as (43), shown at the top of this page, where $\psi_{\mu_\mathrm{TR}}(jv)$ is the CF of μ_TR given in (18). Given that $\psi_\mathrm{J}(jv)$ is the CF of α_J^2, $g_{\mathrm{TR},d_0=+1}(jv)$ in (43) is defined as follows:

$$\begin{aligned}g_{\mathrm{TR},d_0=+1}(jv)&\triangleq\frac{-jv}{1+jv}\cdot\frac{N_\mathrm{s}J_0T}{2N_0}\Big[1+\cos(2\pi f_\mathrm{J}T_\mathrm{r})\Big]\\ &\quad+\frac{jv}{1-jv}\cdot\frac{N_\mathrm{s}J_0T}{2N_0}\Big[1-\cos(2\pi f_\mathrm{J}T_\mathrm{r})\Big].\end{aligned}\tag{44}$$

In the absence of NBI or when $J_0=0$, (43) gives us an alternative, but equivalent, expression to (21) for the BEP of TR signaling with an AcR.[15]

From (16), we can observe that $U_{j|d_0=-1}$, when conditioned on Ψ, is also the difference of two noncentral chi-squared

[14] The mean and variance of a non-central chi-squared r.v. are given by $(k+\mu)$ and $2(k+2\mu)$ respectively, where k is the degrees of freedom and μ is the non-centrality parameter.

[15] Note that the difference in the expressions lies in the fact that we have used the inversion theorem [58], [59] to derive $\mathbb{P}\{Z_\mathrm{TR}\le 0|d_0=+1\}$ in (43).

$$\mu_{\mathrm{TR},Y_3}^{(\mathrm{NBI})} \approx \frac{E_\mathrm{s}}{N_0}\sum_{l=1}^{L_{\mathrm{CAP}}}\alpha_l^2 + \frac{\alpha_\mathrm{J}^2 N_\mathrm{s} J_0 T}{2N_0} - \frac{\alpha_\mathrm{J}^2 N_\mathrm{s} J_0 T}{2N_0}\cos(2\pi f_\mathrm{J} T_\mathrm{r}) + \frac{4\alpha_\mathrm{J}|\widehat{P}(f_\mathrm{J})|\sqrt{2E_\mathrm{p}J_0}\sin(-\pi f_\mathrm{J} T_\mathrm{r})}{N_0}\sum_{j=0}^{\frac{N_\mathrm{s}}{2}-1} a_j \sum_{l=1}^{L_{\mathrm{CAP}}}\alpha_l \sin\left(2\pi f_\mathrm{J}\left(\tau_l + j2T_\mathrm{f} + c_j T_\mathrm{p} + T_\mathrm{r}/2\right) + \varphi\right), \quad (45)$$

r.v.'s with same degrees of freedom, but with different non-centrality parameters. Following the derivation from (38) to (42), we can again resort to the quasi-analytical method to evaluate $\mathbb{P}\{Z_{\mathrm{TR}} > 0 | d_0 = -1\}$. We first derive the non-centrality parameters of Y_3 and Y_4 in (17) conditioned on Ψ, as shown in (45) (at the top of this page) and (46), respectively:

$$\mu_{\mathrm{TR},Y_4}^{(\mathrm{NBI})} \approx \frac{\alpha_\mathrm{J}^2 N_\mathrm{s} J_0 T}{2N_0} + \frac{\alpha_\mathrm{J}^2 N_\mathrm{s} J_0 T}{2N_0}\cos(2\pi f_\mathrm{J} T_\mathrm{r}), \quad (46)$$

where the detailed derivation and the justification of the approximations leading to (45) and (46) can be found in Appendix II. We then replace $\mu_{\mathrm{TR},Y_1}^{(\mathrm{NBI})}$ and $\mu_{\mathrm{TR},Y_2}^{(\mathrm{NBI})}$ in (42) with $\mu_{\mathrm{TR},Y_3}^{(\mathrm{NBI})}$ and $\mu_{\mathrm{TR},Y_4}^{(\mathrm{NBI})}$ to obtain $\mathbb{P}\{Z_{\mathrm{TR}} > 0 | d_0 = -1\}$. Alternatively, under the approximate analytical method leading to (43) and (44) when the dependence of $\mu_{\mathrm{TR},Y_3}^{(\mathrm{NBI})}$ on φ, $\{c_j\}$ and $\{a_j\}$ is negligible, we can ignore the last term in (45). The approximate BEP conditioned on $d_0 = -1$ is then given by

$$\mathbb{P}\{Z_{\mathrm{TR}} > 0 | d_0 = -1\} \simeq P_\mathrm{e}^{(\mathrm{NBI})}\Big(\psi_{\mu_{\mathrm{TR}}}(jv), \psi_\mathrm{J}\left(g_{\mathrm{TR},d_0=-1}(jv)\right), q_{\mathrm{TR}}\Big), \quad (47)$$

where $g_{\mathrm{TR},d_0=-1}(jv)$ in (47) is defined as follows:

$$g_{\mathrm{TR},d_0=-1}(jv) \triangleq \frac{-jv}{1+jv}\cdot\frac{N_\mathrm{s} J_0 T}{2N_0}\Big[1-\cos(2\pi f_\mathrm{J} T_\mathrm{r})\Big] + \frac{jv}{1-jv}\cdot\frac{N_\mathrm{s} J_0 T}{2N_0}\Big[1+\cos(2\pi f_\mathrm{J} T_\mathrm{r})\Big]. \quad (48)$$

Using (43) and (47), it follows that the approximate BEP of TR signaling with an AcR in the presence of NBI is given by

$$P_{\mathrm{e,TR}}^{(\mathrm{NBI})} \simeq \frac{1}{2}\Big[P_\mathrm{e}^{(\mathrm{NBI})}\Big(\psi_{\mu_{\mathrm{TR}}}(jv), \psi_\mathrm{J}\left(g_{\mathrm{TR},d_0=+1}(jv)\right), q_{\mathrm{TR}}\Big) + P_\mathrm{e}^{(\mathrm{NBI})}\Big(\psi_{\mu_{\mathrm{TR}}}(jv), \psi_\mathrm{J}\left(g_{\mathrm{TR},d_0=-1}(jv)\right), q_{\mathrm{TR}}\Big)\Big]. \quad (49)$$

Note that the fidelity of the above approximation depends on the insignificance of the last terms in both $\mu_{\mathrm{TR},Y_1}^{(\mathrm{NBI})}$ and $\mu_{\mathrm{TR},Y_3}^{(\mathrm{NBI})}$. As shown in Appendix I and in Section VI, the approximation is in good agreement with the quasi-analytical results for cases of practical interest.[16]

B. *Differential Transmitted-Reference*

Following the sampling expansion approach and incorporating the NBI in (35), we can rewrite U_j in (24) as

$$U_j = \frac{1}{2W}\sum_{m=1}^{2WT}\Big[d_0 w_{j,m}^2 + e_{-1}w_{j,m}(\xi_{2,j,m}+\eta_{2,j,m}) + e_0 w_{j,m}(\xi_{1,j,m}+\eta_{1,j,m}) + (\xi_{1,j,m}+\eta_{1,j,m})(\xi_{2,j,m}+\eta_{2,j,m})\Big], \quad (50)$$

where $\xi_{1,j,m}$ and $\xi_{2,j,m}$, for odd m (even m) are the real (imaginary) parts of the samples of the equivalent low-pass version of $\xi_{1,j}(t) \triangleq J(t+jT_\mathrm{f}+c_jT_\mathrm{p}-N_\mathrm{s}T_\mathrm{f})$ and $\xi_{2,j}(t) \triangleq J(t+jT_\mathrm{f}+c_jT_\mathrm{p})$, respectively, in the interval $[0,T]$, and the rest of the terms in (50) are defined similarly as in (24). Conditioned on d_0, we can rewrite (50) in the form of (15) and (16), where $\beta_{1,j,m} = \frac{1}{2\sqrt{2W}}(e_{-1}\eta_{2,j,m} + e_{-1}\xi_{2,j,m} + e_0\eta_{1,j,m} + e_0\xi_{1,j,m})$ and $\beta_{2,j,m} = \frac{1}{2\sqrt{2W}}(e_{-1}\eta_{2,j,m} + e_{-1}\xi_{2,j,m} - e_0\eta_{1,j,m} - e_0\xi_{1,j,m})$. Further conditioning on θ, α_J, $\{c_j\}$, and $d_0 = +1$, the conditional variance σ_{DTR}^2 of $\beta_{1,j,m}$ and $\beta_{1,j,m}$ is $\frac{N_0}{4}$.[17] Following the discussion for TR signaling, we will develop the approximate analytical method below. Under the approximation presented in Appendix I, the conditional non-centrality parameters of Y_1 and Y_2 in (17) are given by

$$\mu_{\mathrm{DTR},Y_1}^{(\mathrm{NBI})} \approx \frac{2E_\mathrm{s}}{N_0}\sum_{l=1}^{L_{\mathrm{CAP}}}\alpha_l^2 + \frac{\alpha_\mathrm{J}^2 N_\mathrm{s} J_0 T}{N_0} + \frac{\alpha_\mathrm{J}^2 N_\mathrm{s} J_0 T}{N_0}\cos(2\pi f_\mathrm{J} N_\mathrm{s} T_\mathrm{f}), \quad (51)$$

$$\mu_{\mathrm{DTR},Y_2}^{(\mathrm{NBI})} \approx \frac{\alpha_\mathrm{J}^2 N_\mathrm{s} J_0 T}{N_0} - \frac{\alpha_\mathrm{J}^2 N_\mathrm{s} J_0 T}{N_0}\cos(2\pi f_\mathrm{J} N_\mathrm{s} T_\mathrm{f}). \quad (52)$$

The conditional non-centrality parameters of Y_3 and Y_4 in (17) are given by

$$\mu_{\mathrm{DTR},Y_3}^{(\mathrm{NBI})} \approx \frac{2E_\mathrm{s}}{N_0}\sum_{l=1}^{L_{\mathrm{CAP}}}\alpha_l^2 + \frac{\alpha_\mathrm{J}^2 N_\mathrm{s} J_0 T}{N_0} - \frac{\alpha_\mathrm{J}^2 N_\mathrm{s} J_0 T}{N_0}\cos(2\pi f_\mathrm{J} N_\mathrm{s} T_\mathrm{f}), \quad (53)$$

$$\mu_{\mathrm{DTR},Y_4}^{(\mathrm{NBI})} \approx \frac{\alpha_\mathrm{J}^2 N_\mathrm{s} J_0 T}{N_0} + \frac{\alpha_\mathrm{J}^2 N_\mathrm{s} J_0 T}{N_0}\cos(2\pi f_\mathrm{J} N_\mathrm{s} T_\mathrm{f}), \quad (54)$$

where the above derivations follow straightforwardly from Appendix I and II. Using (51) to (54), the approximate BEP

[16]However, in cases when this approximation fails, we can always resort to the quasi-analytical method.

[17]Note that this conditional variance σ_{DTR}^2 remains the same even when $d_0 = -1$.

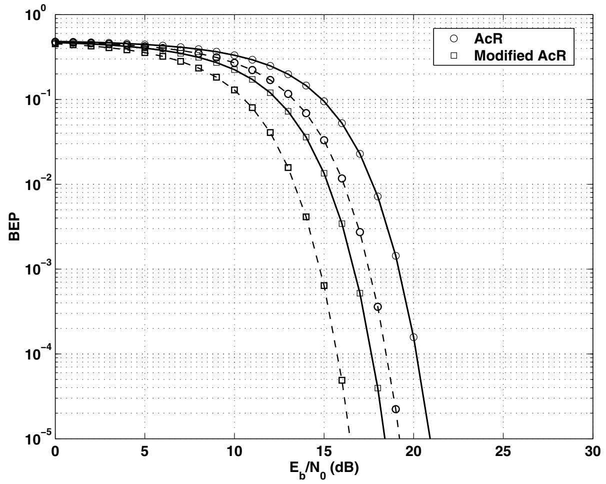

Fig. 3. BEP performance of TR and DTR signaling with an AcR and a modified AcR for $(L, \epsilon, m) = (32, 0, 3)$ and $WT = L$. The solid and dashed lines indicate the TR and DTR signaling, respectively.

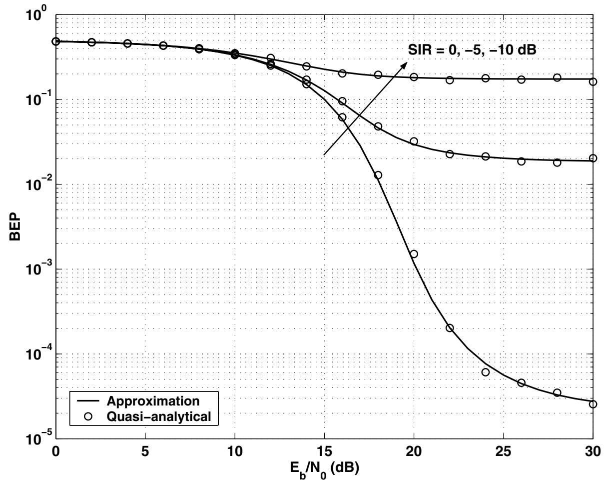

Fig. 4. BEP performance of TR signaling with an AcR in the presence of NBI for $(L, \epsilon, m) = (32, 0, 3)$ and $WT = L$.

of DTR signaling with an AcR in the presence of NBI is then given by

$$P_{\mathrm{e,DTR}}^{(\mathrm{NBI})} \simeq \frac{1}{2}\Big[P_{\mathrm{e}}^{(\mathrm{NBI})}\Big(\psi_{\mu_{\mathrm{DTR}}}(jv), \psi_{\mathrm{J}}\left(g_{\mathrm{DTR},d_0=+1}(jv)\right), q_{\mathrm{DTR}}\Big) + P_{\mathrm{e}}^{(\mathrm{NBI})}\Big(\psi_{\mu_{\mathrm{DTR}}}(jv), \psi_{\mathrm{J}}\left(g_{\mathrm{DTR},d_0=-1}(jv)\right), q_{\mathrm{DTR}}\Big)\Big], \quad (55)$$

where $\psi_{\mu_{\mathrm{DTR}}}(jv)$ is the CF of μ_{DTR} defined after (28), $g_{\mathrm{DTR},d_0=+1}(jv)$ and $g_{\mathrm{DTR},d_0=-1}(jv)$ are defined as follows:

$$g_{\mathrm{DTR},d_0=+1}(jv) \triangleq \frac{-jv}{1+jv}\cdot\frac{N_{\mathrm{s}}J_0T}{N_0}\Big[1+\cos(2\pi f_{\mathrm{J}}N_{\mathrm{s}}T_{\mathrm{f}})\Big] + \frac{jv}{1-jv}\cdot\frac{N_{\mathrm{s}}J_0T}{N_0}\Big[1-\cos(2\pi f_{\mathrm{J}}N_{\mathrm{s}}T_{\mathrm{f}})\Big], \quad (56)$$

$$g_{\mathrm{DTR},d_0=-1}(jv) \triangleq \frac{-jv}{1+jv}\cdot\frac{N_{\mathrm{s}}J_0T}{N_0}\Big[1-\cos(2\pi f_{\mathrm{J}}N_{\mathrm{s}}T_{\mathrm{f}})\Big] + \frac{jv}{1-jv}\cdot\frac{N_{\mathrm{s}}J_0T}{N_0}\Big[1+\cos(2\pi f_{\mathrm{J}}N_{\mathrm{s}}T_{\mathrm{f}})\Big]. \quad (57)$$

We remark that (49) and (55) can be evaluated for a broad class of fading channels, including Nakagami, Rice, and Rayleigh, whose CFs are known in closed-form [58].

VI. Numerical Examples

In this section, we evaluate the performance of both TR and DTR signaling, with and without NBI, based on the unified analysis developed in previous sections. We consider a band-pass UWB system with pulse duration $T_{\mathrm{p}} = 0.5$ ns, average repetition period $T_{\mathrm{f}} = 100$ ns, and $N_{\mathrm{s}} = 16$. For simplicity, T_{r} is set such that there is no ISI or isi in the system, i.e., $T_{\mathrm{r}} = 2T_{\mathrm{f}} - T_{\mathrm{g}} - N_{\mathrm{h}}T_{\mathrm{p}}$. We consider a TH sequence of all ones ($c_j = 1$ for all j) and $N_{\mathrm{h}} = 2$. The NBI carrier frequency is $f_{\mathrm{J}} = 2.45$ GHz.[18] Since the NBI experiences flat Rayleigh fading, the CF of α_{J}^2 is $\psi_{\mathrm{J}}(jv) = 1/(1-jv)$. For UWB channels, it has been verified experimentally that the multipath gains can be modeled as Nakagami-m r.v.'s [8]. As a result, we consider a dense resolvable multipath channel, where each multipath gain is Nakagami distributed with fading severity index m and average power $\mathbb{E}\left\{\alpha_l^2\right\}$, where $\mathbb{E}\left\{\alpha_l^2\right\} = \mathbb{E}\left\{\alpha_1^2\right\}\exp\left[-\epsilon(l-1)\right]$, for $l = 1, \ldots, L$, are normalized such that $\sum_{l=1}^{L}\mathbb{E}\left\{\alpha_l^2\right\} = 1$. For simplicity, the fading severity index m is assumed to be identical for all paths. The average power of the first arriving multipath component is given by $\mathbb{E}\left\{\alpha_1^2\right\}$, and ϵ is the power decay factor. With this model, we consider two sets of parameters, $(L, \epsilon, m) = (32, 0, 3)$ for uniform PDP and $(32, 0.4, 3)$ for exponential PDP.

Figure 3 compares the BEP performance of TR and DTR signaling with an AcR and a modified AcR for $(L, \epsilon, m) = (32, 0, 3)$ and $WT = L$ in the absence of NBI. The difference between TR and DTR signaling is about 2 dB, slightly less than the 3 dB expected from the doubling of the non-centrality parameter shown in Table I. This loss of 1 dB can be attributed to more noise accumulation as $q_{\mathrm{DTR}} = 2q_{\mathrm{TR}}$. Note that the optimum WT is L for uniform PDP [39]. However, when the PDP is exponential, the optimum WT is much smaller than L, and the degradation due to excessive noise accumulation is less significant, as apparent in Fig. 7. By comparing the performance between an AcR and a modified AcR, it can be observed in Fig. 3 that the modified AcR performs better than the AcR by about 3 dB for both signaling schemes. This accounts for the increase of about a factor of two in the instantaneous received SNR through the non-centrality parameter when a modified AcR is used, as indicated in Table I.

To better understand the validity of the approximation developed in Section V, we compare the BEP performance of TR signaling with an AcR in the presence of NBI when $a_j = 1$ for all j and $|\widehat{P}(f_{\mathrm{J}})| \approx \sqrt{T_{\mathrm{p}}}$.[19] Fig. 4 shows the BEP performance of TR signaling for different SIR values, $(L, \epsilon, m) = (32, 0, 3)$ and $WT = L$. It can be observed that

[18] For our numerical results, we assume that the NBI is within the band of interest.

[19] For simplicity, we have considered the case where the frequency response of $p(t)$ is flat over the bandwidth W.

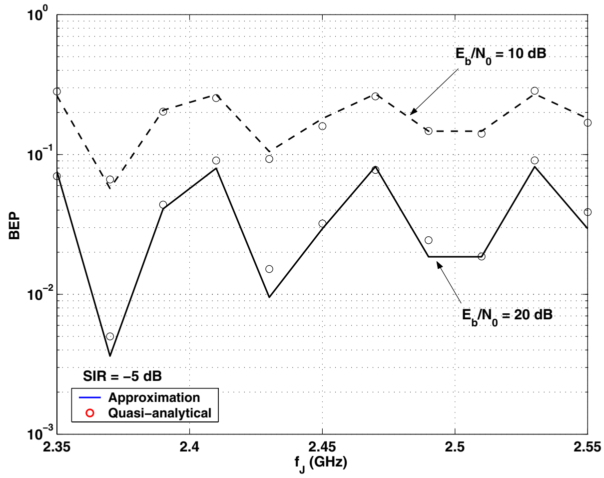

Fig. 5. Effect of NBI carrier frequency on BEP performance of TR signaling with an AcR for $(L, \epsilon, m) = (32, 0, 3)$ and $WT = L$.

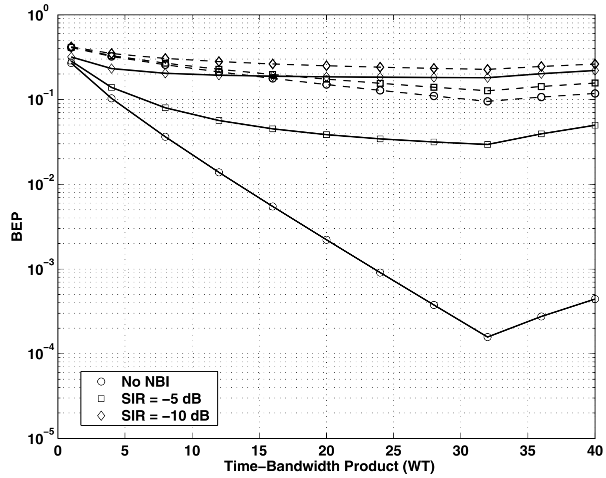

Fig. 6. Effect of integration interval T on BEP performance of TR signaling with an AcR for uniform PDP. The solid and dashed lines indicate $E_{\rm b}/N_0 =$ 20 dB and $E_{\rm b}/N_0 = 15$ dB, respectively.

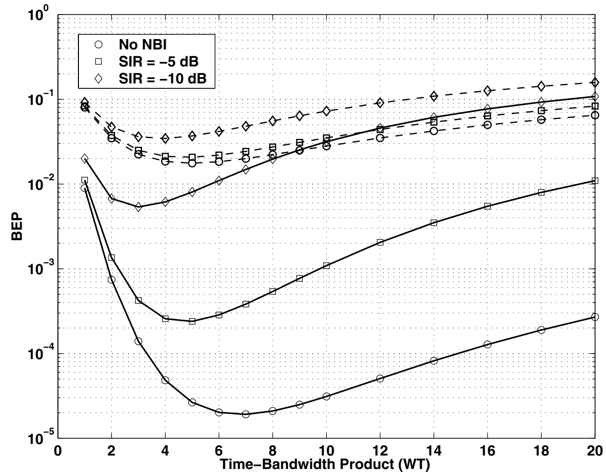

Fig. 7. Effect of integration interval T on BEP performance of TR signaling with an AcR for exponential PDP. The solid and dashed lines indicate $E_{\rm b}/N_0 = 20$ dB and $E_{\rm b}/N_0 = 15$ dB, respectively.

the approximate analytical results are in good agreement with the quasi-analytical results. We further investigate the effect of the NBI carrier frequency on the fidelity of the approximation in Fig. 5 for $(L, \epsilon, m) = (32, 0, 3)$, $WT = L$, and SIR = -5 dB. Similar to the results in Fig. 4, the approximate analytical method is in good agreement with the quasi-analytical results, showing the usefulness of the approximation for investigating the performance of TR signaling schemes in the presence of NBI.

To understand the effect of NBI and PDP on the choice of integration interval T of an AcR, we first plot the BEP of TR signaling in Fig. 6 as a function of time-bandwidth product, WT, using an analytical approximation for $(L, \epsilon, m) = (32, 0, 3)$. Fig. 6 shows that with this PDP, the optimum T is always equal to $T_{\rm g}$ (i.e., $WT = L$), regardless of the presence of NBI. It can also be observed that the performance gain for using the optimum T is significant in the absence of NBI, especially at high $E_{\rm b}/N_0$. This is because, in the absence of NBI, more useful energy is captured with increasing WT until optimum WT is reached for high $E_{\rm b}/N_0$. However, in the presence of NBI, interference energy is also accumulated for every increase in WT, causing performance degradation. This trade-off is more subtle for channels with non-uniform PDP, as illustrated in Fig. 7 for $(L, \epsilon, m) = (32, 0.4, 3)$. It can be seen that the optimum T is no longer at $T_{\rm g}$, since the gain from collecting more residual multipath energies inherent in the channel with exponential PDP is not sufficient to compensate for the noise accumulation beyond the optimum point. Moreover, we observe that the optimum T increases with $E_{\rm b}/N_0$ and SIR, due to decreasing noise and interference accumulation. In general, the optimum T depends on the channel PDP, the operating $E_{\rm b}/N_0$, and the SIR. Consequently, it is important that the AcR is designed with an appropriate choice of T. Some of our work in this direction is reported in [60].

The effect of NBI on TR and DTR signaling with an AcR is plotted in Fig. 8 for different SIR values, $(L, \epsilon, m) = (32, 0.4, 3)$, and optimum T chosen for each $E_{\rm b}/N_0$ and SIR. First, we can observe that the error floor for large values of $E_{\rm b}/N_0$ becomes more significant as SIR decreases for both signaling schemes. In the absence of NBI, DTR signaling has a gain of about 3 dB compared to TR signaling. However, this gain diminishes as SIR decreases. After certain points (e.g, $E_{\rm b}/N_0$ = 20, 16, 10 dB for SIR = -5, -10, -20 dB, respectively), DTR signaling performs worse than TR signaling, as indicated by the error floor. In the interference-limited regime, it is particularly interesting to observe that TR signaling is more robust against NBI compared to DTR signaling. This is because interference is more severe in DTR signaling due to the presence of more noise and interference terms as $q_{\rm DTR} = 2q_{\rm TR}$. Despite a doubling of the received multipath energies in DTR signaling compared to TR signaling, the presence of more interference terms essentially outweighs this gain, as indicated by the crossing of the curves in Fig. 8.

VII. Conclusion

In this paper, we developed an analytical framework and provided a unified performance analysis of TR and DTR signaling for both an AcR and a modified AcR in dense resolvable multipath channels. The framework is based on the sampling expansion approach without the conventional

$$\mu_{\mathrm{TR},Y_1}^{(\mathrm{NBI})} = \underbrace{\frac{1}{2\sigma_{\mathrm{TR}}^2}\sum_{j=0}^{\frac{N_\mathrm{s}}{2}-1}\int_0^T w_j^2(t)dt}_{\triangleq\mu_\mathrm{A}} + \underbrace{\frac{1}{8\sigma_{\mathrm{TR}}^2}\sum_{j=0}^{\frac{N_\mathrm{s}}{2}-1}\int_0^T \left(\xi_{1,j}(t)+\xi_{2,j}(t)\right)^2 dt}_{\triangleq\mu_\mathrm{B}} + \underbrace{\frac{1}{2\sigma_{\mathrm{TR}}^2}\sum_{j=0}^{\frac{N_\mathrm{s}}{2}-1}\int_0^T w_j(t)\left(\xi_{1,j}(t)+\xi_{2,j}(t)\right)dt}_{\triangleq\mu_\mathrm{C}}, \quad (58)$$

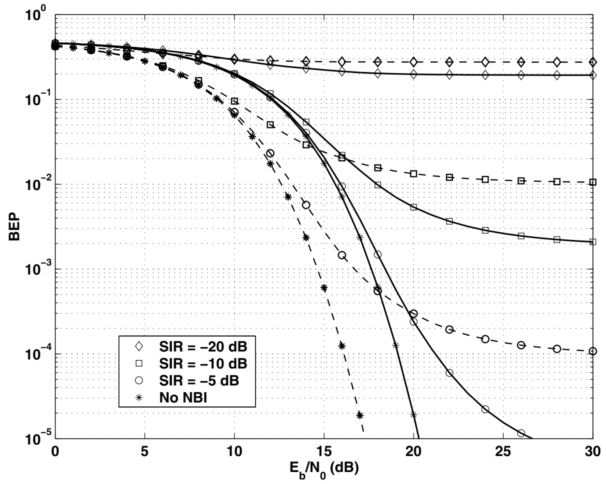

Fig. 8. Effect of NBI on BEP performance of TR and DTR signaling with an AcR for $(L, \epsilon, m) = (32, 0.4, 3)$ and optimum T chosen for each SNR and SIR. The solid and dashed lines indicate the TR and DTR signaling, respectively.

Gaussian approximation, and is valid for a broad class of fading channels. We first analyzed the case without NBI, then extended our analysis to take into account the effect of NBI. We developed a quasi-analytical method as well as an approximate analytical method to evaluate the BEP of TR and DTR signaling in the presence of NBI. We showed that the approximate analytical method is particularly useful in obtaining BEP expressions that provide insight into the effect of NBI on the performance of TR signaling schemes. Numerical results revealed that the approximation is in good agreement with the quasi-analytical results. We quantified the effects of NBI and channel PDP on the optimum integration interval of an AcR, showing that NBI imposes a practical limit on the amount of multipath energy that can be captured by an AcR. In particular, we showed that the optimum integration interval strongly depends on the channel PDP and the SNR, as well as the SIR. We compared TR and DTR signaling in terms of their sensitivity to NBI and revealed that the BEP improvement provided by DTR signaling is entirely different in noise-limited and interference-limited regimes.

Acknowledgment

The authors gratefully acknowledge W. M. Gifford, J. Lien, and W. Suwansantisuk for insightful comments and careful reading of the manuscript. They would also like to thank the Editor and the anonymous reviewers for helpful suggestions.

Appendix I
Derivation of $\mu_{\mathrm{TR},Y_1}^{(\mathrm{NBI})}$ and $\mu_{\mathrm{TR},Y_2}^{(\mathrm{NBI})}$

In this appendix, the derivation of the non-centrality parameters $\mu_{\mathrm{TR},Y_1}^{(\mathrm{NBI})}$ in (38) and $\mu_{\mathrm{TR},Y_2}^{(\mathrm{NBI})}$ in (39) are shown. We begin first with the derivation of $\mu_{\mathrm{TR},Y_1}^{(\mathrm{NBI})}$ in (58) as shown at the top of this page, where we can simplify μ_A and μ_B as

$$\mu_\mathrm{A} = \frac{1}{2\sigma_{\mathrm{TR}}^2}\sum_{j=0}^{\frac{N_\mathrm{s}}{2}-1}\int_0^T w_j^2(t)dt = \frac{E_\mathrm{s}}{N_0}\sum_{l=1}^{L_{\mathrm{CAP}}}\alpha_l^2,$$
$$\mu_\mathrm{B} \approx \frac{\alpha_\mathrm{J}^2 N_\mathrm{s} J_0 T}{2N_0} + \frac{\alpha_\mathrm{J}^2 N_\mathrm{s} J_0 T}{2N_0}\cos(2\pi f_\mathrm{J} T_\mathrm{r}). \quad (59)$$

To obtain μ_B in (59), we simply need to expand all the terms of μ_B in (58) as follows:

$$\frac{1}{8\sigma_{\mathrm{TR}}^2}\sum_{j=0}^{\frac{N_\mathrm{s}}{2}-1}\int_0^T \xi_{1,j}^2(t)dt$$
$$= \frac{\alpha_\mathrm{J}^2 J_0}{2N_0}\sum_{j=0}^{\frac{N_\mathrm{s}}{2}-1}\Bigg[T + \frac{\sin\left(4\pi f_\mathrm{J}(T + j2T_\mathrm{f} + c_j T_\mathrm{p}) + 2\theta\right)}{4\pi f_\mathrm{J}} - \frac{\sin\left(4\pi f_\mathrm{J}(j2T_\mathrm{f} + c_j T_\mathrm{p}) + 2\theta\right)}{4\pi f_\mathrm{J}}\Bigg] \approx \frac{\alpha_\mathrm{J}^2 N_\mathrm{s} J_0 T}{4N_0}$$

$$\frac{1}{8\sigma_{\mathrm{TR}}^2}\sum_{j=0}^{\frac{N_\mathrm{s}}{2}-1}\int_0^T \xi_{2,j}^2(t)dt \approx \frac{\alpha_\mathrm{J}^2 N_\mathrm{s} J_0 T}{4N_0}$$

where we have made the above approximations by observing that $T \gg \frac{1}{4\pi f_\mathrm{J}}$ and $|\sin(\phi)| \leq 1$. In addition,

$$\frac{1}{4\sigma_{\mathrm{TR}}^2}\sum_{j=0}^{\frac{N_\mathrm{s}}{2}-1}\int_0^T \xi_{1,j}(t)\xi_{2,j}(t)dt \approx \mu_\mathrm{D}. \quad (60)$$

where $\mu_\mathrm{D} = \frac{\alpha_\mathrm{J}^2 N_\mathrm{s} J_0 T}{2N_0}\cos(2\pi f_\mathrm{J} T_\mathrm{r})$ when $T\cos(2\pi f_\mathrm{J} T_\mathrm{r}) \gg \frac{1}{4\pi f_\mathrm{J}}$. Otherwise, μ_D is on the same order as $\frac{1}{4\pi f_\mathrm{J}}$, which is negligible compared to the first term of μ_B in (59). As a result, we can ignore the latter case and consider only the scenario when $T\cos(2\pi f_\mathrm{J} T_\mathrm{r}) \gg \frac{1}{4\pi f_\mathrm{J}}$ as shown in (59). Next, we can rewrite μ_C in (58) as (61) shown at the top of next page, where $|\widehat{P}(f_\mathrm{J})|$ is the magnitude of the frequency response of $p(t)$ at frequency f_J. The composite random phase is given by $\varphi \triangleq \arg\{\widehat{P}(f_\mathrm{J})\} + \theta$, where $\arg\{\widehat{P}(f_\mathrm{J})\}$ is the angle of the frequency response of $p(t)$ at frequency f_J, and φ is uniformly distributed over $[0, 2\pi)$. In summary, we obtain $\mu_{\mathrm{TR},Y_1}^{(\mathrm{NBI})}$ in (38) using (59) and (61).

Using (58), (59) and (61), we can determine the validity of the approximate analytical method using (62) and (63) shown at the top of the next page. For a given set of system parameters, we simply need to check if $\mu_\mathrm{A} + \mu_\mathrm{B} \gg \mu_\mathrm{C}$ using (62) and (63). For example, this can arise when Walsh-Hadamard sequences are used for $\{a_j\}$. To elaborate on this example, we first numerically average (over $\{\alpha_l\}$ and α_J) the quantities within $|\cdot|$ of (62) and (63) for a typical set of system parameters ($T_\mathrm{f} = 100$ns, $T_\mathrm{p} = 0.5$ns, $T_\mathrm{r} = 40$ns, possible

$$\mu_{\mathrm{C}} = \frac{2\alpha_{\mathrm{J}}\sqrt{2E_{\mathrm{p}}J_0}}{N_0}\sum_{j=0}^{\frac{N_{\mathrm{s}}}{2}-1} a_j \sum_{l=1}^{L_{\mathrm{CAP}}} \alpha_l \int_0^{T_{\mathrm{p}}} p(t) \times \left[\cos\left(2\pi f_{\mathrm{J}}(t+\tau_l+j2T_{\mathrm{f}}+c_jT_{\mathrm{p}})+\theta\right)+\cos\left(2\pi f_{\mathrm{J}}(t+\tau_l+j2T_{\mathrm{f}}+c_jT_{\mathrm{p}}+T_{\mathrm{r}})+\theta\right)\right] dt$$
$$= \frac{4\alpha_{\mathrm{J}}|\widehat{P}(f_{\mathrm{J}})|\sqrt{2E_{\mathrm{p}}J_0}\cos\left(\pi f_{\mathrm{J}}T_{\mathrm{r}}\right)}{N_0}\sum_{j=0}^{\frac{N_{\mathrm{s}}}{2}-1} a_j \sum_{l=1}^{L_{\mathrm{CAP}}} \alpha_l \cos\left(2\pi f_{\mathrm{J}}\left(\tau_l+j2T_{\mathrm{f}}+c_jT_{\mathrm{p}}+T_{\mathrm{r}}/2\right)+\varphi\right), \quad (61)$$

$$\frac{\mu_{\mathrm{A}}}{\mu_{\mathrm{C}}} = \left|\frac{\sum_{l=1}^{L_{\mathrm{CAP}}}\alpha_l^2}{\alpha_{\mathrm{J}}\cos\left(\pi f_{\mathrm{J}}T_{\mathrm{r}}\right)\sum_{j=0}^{\frac{N_{\mathrm{s}}}{2}-1} a_j \sum_{l=1}^{L_{\mathrm{CAP}}}\alpha_l\cos\left(2\pi f_{\mathrm{J}}\left(\tau_l+j2T_{\mathrm{f}}+c_jT_{\mathrm{p}}+\frac{T_{\mathrm{r}}}{2}\right)+\varphi\right)}\right|\frac{N_{\mathrm{s}}}{4|\widehat{P}(f_{\mathrm{J}})|}\sqrt{\frac{T_{\mathrm{f}}\mathsf{SIR}}{2}}, \quad (62)$$

$$\frac{\mu_{\mathrm{B}}}{\mu_{\mathrm{C}}} = \left|\frac{\alpha_{\mathrm{J}}\cos(\pi f_{\mathrm{J}}T_{\mathrm{r}})}{\sum_{j=0}^{\frac{N_{\mathrm{s}}}{2}-1} a_j \sum_{l=1}^{L_{\mathrm{CAP}}}\alpha_l\cos\left(2\pi f_{\mathrm{J}}\left(\tau_l+j2T_{\mathrm{f}}+c_jT_{\mathrm{p}}+\frac{T_{\mathrm{r}}}{2}\right)+\varphi\right)}\right|\frac{N_{\mathrm{s}}L_{\mathrm{CAP}}T_{\mathrm{p}}}{4|\widehat{P}(f_{\mathrm{J}})|}\sqrt{\frac{1}{2T_{\mathrm{f}}\mathsf{SIR}}}, \quad (63)$$

$$\mu_{\mathrm{TR},Y_3}^{(\mathrm{NBI})} = \frac{1}{2\sigma_{\mathrm{TR}}^2}\sum_{j=0}^{\frac{N_{\mathrm{s}}}{2}-1}\int_0^T w_j^2(t)dt + \frac{1}{8\sigma_{\mathrm{TR}}^2}\sum_{j=0}^{\frac{N_{\mathrm{s}}}{2}-1}\int_0^T\left(\xi_{2,j}(t)-\xi_{1,j}(t)\right)^2 dt + \frac{1}{2\sigma_{\mathrm{TR}}^2}\sum_{j=0}^{\frac{N_{\mathrm{s}}}{2}-1}\int_0^T w_j(t)\left(\xi_{2,j}(t)-\xi_{1,j}(t)\right) dt$$
$$\approx \frac{E_{\mathrm{s}}}{N_0}\sum_{l=1}^{L_{\mathrm{CAP}}}\alpha_l^2 + \frac{\alpha_{\mathrm{J}}^2N_{\mathrm{s}}J_0T}{2N_0} - \frac{\alpha_{\mathrm{J}}^2N_{\mathrm{s}}J_0T}{2N_0}\cos(2\pi f_{\mathrm{J}}T_{\mathrm{r}})$$
$$+\frac{4\alpha_{\mathrm{J}}|\widehat{P}(f_{\mathrm{J}})|\sqrt{2E_{\mathrm{p}}J_0}\sin\left(-\pi f_{\mathrm{J}}T_{\mathrm{r}}\right)}{N_0}\sum_{j=0}^{\frac{N_{\mathrm{s}}}{2}-1} a_j\sum_{l=1}^{L_{\mathrm{CAP}}}\alpha_l\sin\left(2\pi f_{\mathrm{J}}\left(\tau_l+j2T_{\mathrm{f}}+c_jT_{\mathrm{p}}+T_{\mathrm{r}}/2\right)+\varphi\right), \quad (65)$$

$f_{\mathrm{J}} = 1.575$ GHz, 3.5 GHz, and 5.745 GHz) and considering $c_j = 1$ for all j and Walsh-Hadamard sequences for $\{a_j\}$. Results have shown that the value of $|\cdot|$ in (62) and (63) is always greater than 1. Approximating these factors by 1 and $|\widehat{P}(f_{\mathrm{J}})| \approx \sqrt{T_{\mathrm{p}}}$, we focus on the rest of the terms in (62) and (63). Since T_{f} is usually on the order of 100 times T_{p}, and N_{s} and L_{CAP} are usually larger than $4\sqrt{2}$, we can verify that $\mu_{\mathrm{A}} + \mu_{\mathrm{B}} \gg \mu_{\mathrm{C}}$ and neglect μ_{C} when $\mathsf{SIR} \geq -20$ dB.

Using similar approach leading to (59), $\mu_{\mathrm{TR},Y_2}^{(\mathrm{NBI})}$ in (39) can be approximated as follows:

$$\mu_{\mathrm{TR},Y_2}^{(\mathrm{NBI})} = \frac{1}{8\sigma_{\mathrm{TR}}^2}\sum_{j=0}^{\frac{N_{\mathrm{s}}}{2}-1}\int_0^T(\xi_{2,j}(t)-\xi_{1,j}(t))^2dt \approx \frac{\alpha_{\mathrm{J}}^2N_{\mathrm{s}}J_0T}{2N_0} - \frac{\alpha_{\mathrm{J}}^2N_{\mathrm{s}}J_0T}{2N_0}\cos(2\pi f_{\mathrm{J}}T_{\mathrm{r}}). \quad (64)$$

APPENDIX II
DERIVATION OF $\mu_{\mathrm{TR},Y_3}^{(\mathrm{NBI})}$ AND $\mu_{\mathrm{TR},Y_4}^{(\mathrm{NBI})}$

In this appendix, the non-centrality parameters $\mu_{\mathrm{TR},Y_3}^{(\mathrm{NBI})}$ in (45) and $\mu_{\mathrm{TR},Y_4}^{(\mathrm{NBI})}$ in (46) are derived. We derive $\mu_{\mathrm{TR},Y_3}^{(\mathrm{NBI})}$ in (65), shown at the top of this page, using similar steps as in Appendix I. Similarly, $\mu_{\mathrm{TR},Y_4}^{(\mathrm{NBI})}$ is given by

$$\mu_{\mathrm{TR},Y_4}^{(\mathrm{NBI})} = \frac{1}{8\sigma_{\mathrm{TR}}^2}\sum_{j=0}^{\frac{N_{\mathrm{s}}}{2}-1}\int_0^T(\xi_{2,j}(t)+\xi_{1,j}(t))^2dt \approx \frac{\alpha_{\mathrm{J}}^2N_{\mathrm{s}}J_0T}{2N_0} + \frac{\alpha_{\mathrm{J}}^2N_{\mathrm{s}}J_0T}{2N_0}\cos(2\pi f_{\mathrm{J}}T_{\mathrm{r}}). \quad (66)$$

REFERENCES

[1] M. Z. Win and R. A. Scholtz, "Impulse radio: How it works," *IEEE Commun. Lett.*, vol. 2, no. 2, pp. 36–38, Feb. 1998.

[2] ——, "Ultra-wide bandwidth time-hopping spread-spectrum impulse radio for wireless multiple-access communications," *IEEE Trans. Commun.*, vol. 48, no. 4, pp. 679–691, Apr. 2000.

[3] P. Withington, H. Fluhler, and S. Nag, "Enhancing homeland security with advanced UWB sensors," *IEEE Microwave Mag.*, vol. 4, no. 3, pp. 51–58, Sept. 2003.

[4] S. Roy, J. R. Foerster, V. S. Somayazulu, and D. G. Leeper, "Ultrawideband radio design: the promise of high-speed, short-range wireless connectivity," *Proc. IEEE*, vol. 92, no. 2, pp. 295–311, Feb. 2004.

[5] M. Z. Win and R. A. Scholtz, "On the robustness of ultra-wide bandwidth signals in dense multipath environments," *IEEE Commun. Lett.*, vol. 2, no. 2, pp. 51–53, Feb. 1998.

[6] ——, "On the energy capture of ultra-wide bandwidth signals in dense multipath environments," *IEEE Commun. Lett.*, vol. 2, no. 9, pp. 245–247, Sept. 1998.

[7] ——, "Characterization of ultra-wide bandwidth wireless indoor communications channel: A communication theoretic view," *IEEE J. Select. Areas Commun.*, vol. 20, no. 9, pp. 1613–1627, Dec. 2002.

[8] D. Cassioli, M. Z. Win, and A. F. Molisch, "The ultra-wide bandwidth indoor channel: from statistical model to simulations," *IEEE J. Select. Areas Commun.*, vol. 20, no. 6, pp. 1247–1257, Aug. 2002.

[9] S. Gezici, Z. Tian, G. B. Giannakis, H. Kobayashi, A. F. Molisch, H. V. Poor, and Z. Sahinoglu, "Localization via ultra-wideband radios: a look at positioning aspects for future sensor networks," *IEEE Signal Processing Mag.*, vol. 22, no. 4, pp. 70–84, July 2005.

[10] D. B. Jourdan, D. Dardari, and M. Z. Win, "Position error bound for UWB localization in dense cluttered environments," in *Proc. IEEE Int. Conf. on Commun.*, vol. 8, Istanbul, TURKEY, June 2006, pp. 587–592

[11] D. Dardari and M. Z. Win, "Threshold-based time-of-arrival estimators in UWB dense multipath channels," in *Proc. IEEE Int. Conf. on Commun.*, vol. 10, Istanbul, TURKEY, June 2006, pp. 4723–4728

[12] D. Dardari, C.-C. Chong, and M. Z. Win, "Analysis of threshold-based TOA estimator in UWB channels," in *Proc. of European Signal Processing Conf.*, Florence, ITALY, Sept. 2006.

[13] D. B. Jourdan, D. Dardari, and M. Z. Win, "Position error bound for UWB localization in dense cluttered environments," *IEEE Trans. Aerosp. Electron. Syst.*, 2007, to appear.

[14] C. Falsi, D. Dardari, L. Mucchi, and M. Z. Win, "Time of arrival estimation for UWB localizers in realistic environments," *EURASIP J. Appl. Signal Processing (Special Issue on Wireless Location Technologies and Applications)*, vol. 2006, Article ID 32082, 13 pages, 2006.

[15] M. M. Hämäläinen, R. Tesi, and J. Iianatti, "On the UWB system performance studies in AWGN channel with interference in UMTS band," in *Proc. IEEE Conf. on Ultra Wideband Sys. and Technol.*, Baltimore, MD, May 2002, pp. 321–325.

[16] M. M. Hämäläinen, R. Tesi, J. Iianatti, and V. Hovinen, "On the performance comparison of different UWB data modulation schemes in AWGN channel in the presence of jamming," in *Proc. IEEE Radio and Wireless Conf.*, Boston, MA, Aug. 2002, pp. 83–86.

[17] M. M. Hämäläinen, V. Hovinen, R. Tesi, J. H. J. Iinatti, and M. Latva-aho, "On the UWB system coexistence with GSM900, UMTS/WCDMA, and GPS," *IEEE J. Select. Areas Commun.*, vol. 20, no. 9, pp. 1712–1721, Dec. 2002.

[18] R. Giuliano and F. Mazzenga, "On the coexistence of power-controlled ultrawide-band systems with UMTS, GPS, DCS1800, and fixed wireless systems," *IEEE Trans. Veh. Technol.*, vol. 54, no. 1, pp. 62–81, Jan. 2005.

[19] A. Taha and K. M. Chugg, "A theoretical study on the effects of interference on UWB multiple access impulse radio," in *Proc. Asilomar Conf. on Signals, Systems and Computers*, vol. 1, Pacific Grove, CA, Nov. 2002, pp. 728–732.

[20] J. R. Foerster, "The performance of a Direct Sequence spread ultra-wideband system in the presence of multipath, narrowband interference and multi-user interference," in *Proc. IEEE Conf. on Ultra Wideband Sys. and Technol.*, Baltimore, MD, May 2002, pp. 87–91.

[21] L. Zhao and A. M. Haimovich, "Performance of ultra-wideband communications in the presence of interference," *IEEE J. Select. Areas Commun.*, vol. 20, no. 9, pp. 1684–1691, Dec. 2002.

[22] J. D. Choi and W. E. Stark, "Performance analysis of ultra-wideband spread-spectrum communications in narrowband interference," in *Proc. IEEE Military Commun. Conf.*, vol. 2, Anaheim, CA, Oct. 2002, pp. 1075–1080.

[23] A. Giorgetti, M. Chiani, and M. Z. Win, "The effect of narrowband interference on wideband wireless communication systems," *IEEE Trans. Commun.*, vol. 53, no. 12, pp. 2139–2149, Dec. 2005.

[24] A. Giorgetti and D. Dardari, "The impact of OFDM interference on TH-PPM/BPAM transmission systems," in *Proc. IEEE Semiannual Veh. Technol. Conf.*, vol. 2, Stockholm, SWEDEN, May 2005, pp. 1037–1042.

[25] C. R. C. M. da Silva and L. B. Milstein, "The effects of narrowband interference on UWB communication systems with imperfect channel estimation," *IEEE J. Select. Areas Commun.*, vol. 24, no. 4, pp. 717–723, Apr. 2006.

[26] Q. Li and L. A. Rusch, "Multiuser detection for DS-CDMA UWB in the home environment," *IEEE J. Select. Areas Commun.*, vol. 20, no. 9, pp. 1701–1711, Dec. 2002.

[27] X. Chu and R. D. Murch, "The effect of NBI on UWB time-hopping systems," *IEEE Trans. Wireless Commun.*, vol. 3, no. 5, pp. 1431–1436, Sept. 2004.

[28] I. Bergel, E. Fishler, and H. Messer, "Narrowband interference mitigation in impulse radio," *IEEE Trans. Commun.*, vol. 53, no. 8, pp. 1278–1282, Aug. 2005.

[29] C. R. C. M. da Silva and L. B. Milstein, "Spectral-encoded UWB communication systems: Real-time implementation and interference suppression," *IEEE Trans. Commun.*, vol. 53, no. 8, pp. 1391–1401, Aug. 2005.

[30] N. Boubaker and K. B. Letaief, "MMSE multipath diversity combining for multi-access TH-UWB in the presence of NBI," *IEEE Trans. Wireless Commun.*, vol. 5, no. 4, pp. 712–719, Apr. 2006.

[31] B. Basore, "Noise-like signals and their detection by correlation," Ph.D. dissertation, MIT, Cambridge, MA, May 1952.

[32] C. K. Rushforth, "Transmitted-reference techniques for random or unknown channels," *IEEE Trans. Inform. Theory*, vol. 10, no. 1, pp. 39–42, Jan. 1964.

[33] R. Gagliardi, "A geometrical study of transmitted reference communication system," *IEEE Trans. Commun.*, vol. 12, no. 4, pp. 118–123, Dec. 1964.

[34] A. Polydoros and K. T. Woo, "LPI detection of frequency-hopping signals using autocorrelation techniques," *IEEE J. Select. Areas Commun.*, vol. 3, no. 5, pp. 714 – 726, Sept. 1985.

[35] W. M. Gifford and M. Z. Win, "On transmitted-reference UWB communications," in *Proc. 38th Asilomar Conf. on Signals, Systems and Computers*, Pacific Grove, CA, Nov. 2004, pp. 1526–1531.

[36] R. Hoctor and H. Tomlinson, "Delay-hopped transmitted-reference RF communications," in *Proc. IEEE Conf. on Ultra Wideband Sys. and Technol.*, Baltimore, MD, June 2002, pp. 265–270.

[37] J. D. Choi and W. E. Stark, "Performance of ultra-wideband communications with suboptimal receivers in multipath channels," *IEEE J. Select. Areas Commun.*, vol. 20, no. 9, pp. 1754–1766, Dec. 2002.

[38] T. Q. S. Quek and M. Z. Win, "Ultrawide bandwidth transmitted-reference signaling," in *Proc. IEEE Int. Conf. on Commun.*, vol. 6, Paris, FRANCE, June 2004, pp. 3409–3413.

[39] ——, "Analysis of UWB transmitted-reference communication systems in dense multipath channels," *IEEE J. Select. Areas Commun.*, vol. 23, no. 9, pp. 1863–1874, Sept. 2005.

[40] Y.-L. Chao and R. A. Scholtz, "Ultra-wideband transmitted reference systems," *IEEE Trans. Veh. Technol.*, vol. 54, no. 5, pp. 1556–1569, Sept. 2005.

[41] W. Suwansantisuk and M. Z. Win, "Fundamental limits on spread spectrum signal acquisition," in *Proc. Conf. on Inform. Sci. and Sys.*, Baltimore, MD, Mar. 2005.

[42] ——, "Optimal search procedures for spread spectrum signal acquisition," in *Proc. Conf. on Inform. Sci. and Sys.*, Baltimore, MD, Mar. 2005.

[43] W. Suwansantisuk, M. Z. Win, and L. A. Shepp, "On the performance of wide-bandwidth signal acquisition in dense multipath channels," *IEEE Trans. Veh. Technol.*, vol. 54, no. 5, pp. 1584–1594, Sept. 2005.

[44] W. Suwansantisuk and M. Z. Win, "Multipath aided rapid acquisition: Optimal search strategies," *IEEE Trans. Inform. Theory*, vol. 53, no. 1, pp. 174–193, Jan. 2007.

[45] T. Q. S. Quek, M. Z. Win, and D. Dardari, "UWB transmitted-reference signaling schemes - Part I: Performance analysis," in *Proc. IEEE Int. Conf. on Ultra-Wideband*, Zürich, SWITZERLAND, Sept. 2005, pp. 587–592.

[46] A. A. D'Amico and U. Mengali, "GLRT receivers for UWB systems," *IEEE Commun. Lett.*, vol. 9, no. 6, pp. 487–489, June 2005.

[47] R. A. Scholtz, "The orgins of spread-spectrum communications," *IEEE Trans. Commun.*, vol. 30, no. 5, pp. 822–854, May 1982.

[48] R. Wilson and R. Scholtz, "Template estimation in ultra-wideband radio," in *Proc. Asilomar Conf. on Signals, Systems and Computers*, vol. 2, Pacific Grove, CA, Nov. 2003, pp. 1244–1248.

[49] M. Pausini and G. J. M. Janssen, "On the narrowband interference in transmitted reference UWB receivers," in *Proc. IEEE Int. Conf. on Ultra-Wideband*, Zürich, SWITZERLAND, Sept. 2005, pp. 571–575.

[50] T. Q. S. Quek, M. Z. Win, and D. Dardari, "UWB transmitted-reference signaling schemes - Part II: Narrowband interference analysis," in *Proc. IEEE Int. Conf. on Ultra-Wideband*, Zürich, SWITZERLAND, Sept. 2005, pp. 593–598.

[51] Y.-L. Chao and R. Scholtz, "Novel UWB transmitted-reference signaling schemes," in *Proc. Asilomar Conf. on Signals, Systems and Computers*, vol. 1, Pacific Grove, CA, Nov. 2004, pp. 652–656.

[52] C.-C. Chong and S. K. Yong, "A generic statistical-based UWB channel model for high-rise apartments," *IEEE Trans. Antennas Propagat.*, vol. 53, no. 8, pp. 2389–2399, Aug. 2005.

[53] C.-C. Chong, Y.-E. Kim, S. K. Yong, and S.-S. Lee, "Statistical characterization of the UWB propagation channel in indoor residential environment," *Wireless Communications and Mobile Computing, Wiley InterScience*, vol. 5, no. 5, pp. 503–512, Aug. 2005.

[54] S. R. Aedudodla, S. Vijayakumaran, and T. F. Wong, "Acquisition of direct-sequence transmitted reference ultra-wideband signals," *IEEE J. Select. Areas Commun.*, vol. 24, no. 4, pp. 759–765, Apr. 2006.

[55] N. He and C. Tepedelenlioglu, "Performance analysis of non-coherent UWB receivers at different synchronization levels," *IEEE Trans. Wireless Commun.*, vol. 5, no. 6, pp. 1266–1273, June 2006.

[56] M. Casu and G. Durisi, "Implementation aspects of a transmitted-reference UWB receiver," *Wireless Commun. Mobile Comput.*, vol. 5, no. 5, pp. 537–549, Aug. 2005.

[57] W. M. Gifford, M. Z. Win, and M. Chiani, "Diversity with practical channel estimation," *IEEE Trans. Wireless Commun.*, vol. 4, no. 4, pp. 1935–1947, July 2005.

[58] M. K. Simon and M.-S. Alouini, *Digital Communication over Fading Channels: A Unified Approach to Performance Analysis*, 1st ed. New York, NY, 10158: John Wiley & Sons, Inc., 2000.

[59] J. Gil-Pelaez, "Note on the inversion theorem," *Biometrika*, vol. 38, no. 3, pp. 481–482, Dec. 1951.

[60] D. Dardari, A. Giorgetti, M. Chiani, T. Q. Quek, and M. Z. Win, "A stop-and-go transmitted-reference UWB receiver," in *Proc. IEEE Int. Conf. on Ultra Wideband*, Waltham, MA, Sept. 2006, pp. 587–592.

Tony Q.S. Quek (S'98) received the B.E. and M.E. degrees in electrical and electronics engineering from Tokyo Institute of Technology, Tokyo, Japan, in 1998 and 2000, respectively. From 2001 to 2002, he was with Centre for Wireless Communications, Singapore as a research engineer.

Since 2002, Mr. Quek has been with the Laboratory for Information and Decision Systems (LIDS) at Massachusetts Institute of Technology (MIT), Cambridge, where he is now a Ph.D. candidate. His research interests include wireless communications, information theory, and optimization theory with special emphasis on ultra-wide bandwidth (UWB) systems, and design of robust and efficient wireless networks.

Mr. Quek received the Singapore Government Scholarship in 1993, Tokyu Foundation Fellowship in 1998, and the ASTAR National Science Scholarship in 2002. He served as member of the Technical Program Committee (TPC) for the IEEE International Conference on Communications (ICC) in 2007, the IEEE Conference on Ultra Wideband in 2006, and the IEEE ICC in 2004.

Davide Dardari was born in Rimini, Italy, on January 19, 1968. He received his Laurea degree in Electronic Engineering (*summa cum laude*) and his Ph.D. in Electronic Engineering and Computer Science from the University of Bologna, Italy, in 1993 and 1998, respectively.

He joined the Consorzio Nazionale Interuniversitario per le Telecomunicazioni (CNIT), Italy, in 1998 working on both the experimentation of multimedia services through heterogeneous satellite networks and the design of DSP-based CDMA satellite modems for ASI (Italian Space Agency). From 2000 to 2005, he was a lecturer and a research associate at the Dipartimento di Elettronica, Informatica e Sistemistica (DEIS), University of Bologna. Since 2005, he has been an Associate Professor at the University of Bologna at Cesena, Cesena (FC), Italy. During Spring 2005, he was a research affiliate at Massachusetts Institute of Technology (MIT), Cambridge, USA. His research interests focus on OFDM systems, ultrawide bandwidth communication and localization, wireless sensor networks, and wideband wireless LANs. He has played a significant role in several national and European projects.

He is an active member of the IEEE, where he serves as a reviewer for Transactions/Journals and Conferences, and as a TPC member for several international conferences. He is co-chair of the Wireless Communications Symposium of the 2007 IEEE International Conference on Communications, and was co-chair of the 2006 IEEE International Conference on Ultra-Wideband. Currently, he is an Editor for IEEE TRANSACTIONS ON WIRELESS COMMUNICATIONS, as well as Lead Editor for the EURASIP JOURNAL ON ADVANCES IN SIGNAL PROCESSING (Special Issue on Cooperative Localization in Wireless Ad Hoc and Sensor Networks).

Moe Z. Win (S'85-M'87-SM'97-F'04) received the B.S. degree (*magna cum laude*) from Texas A&M University, College Station, in 1987 and the M.S. degree from the University of Southern California (USC), Los Angeles, in 1989, both in Electrical Engineering. As a Presidential Fellow at USC, he received both an M.S. degree in Applied Mathematics and the Ph.D. degree in Electrical Engineering in 1998.

Dr. Win is an Associate Professor at the Laboratory for Information & Decision Systems (LIDS), Massachusetts Institute of Technology (MIT). Prior to joining MIT, he spent five years at AT&T Research Laboratories and seven years at the Jet Propulsion Laboratory. His main research interests are the applications of mathematical and statistical theories to communication, detection, and estimation problems. Specific current research topics include measurement and modeling of time-varying channels, design and analysis of multiple antenna systems, ultra-wide bandwidth (UWB) systems, optical transmission systems, and space communications systems.

Professor Win has been actively involved in organizing and chairing a number of international conferences. He served as the Technical Program Chair for the IEEE Conference on Ultra Wideband in 2006, the IEEE Communication Theory Symposia of ICC-2004 and Globecom-2000, and the IEEE Conference on Ultra Wideband Systems and Technologies in 2002; Technical Program Vice-Chair for the IEEE International Conference on Communications in 2002; and the Tutorial Chair for the IEEE Semiannual International Vehicular Technology Conference in Fall 2001. He served as the chair (2004-2006) and secretary (2002-2004) for the *Radio Communications Committee* of the IEEE Communications Society. Dr. Win is currently an Editor for IEEE TRANSACTIONS ON WIRELESS COMMUNICATIONS. He served as Area Editor for *Modulation and Signal Design* (2003-2006), Editor for *Wideband Wireless and Diversity* (2003-2006), and Editor for *Equalization and Diversity* (1998-2003), all for the IEEE TRANSACTIONS ON COMMUNICATIONS. He was Guest-Editor for the 2002 IEEE JOURNAL ON SELECTED AREAS IN COMMUNICATIONS (Special Issue on Ultra -Wideband Radio in Multiaccess Wireless Communications).

Professor Win received the International Telecommunications Innovation Award from Korea Electronics Technology Institute in 2002, a Young Investigator Award from the Office of Naval Research in 2003, and the IEEE Antennas and Propagation Society Sergei A. Schelkunoff Transactions Prize Paper Award in 2003. In 2004, Dr. Win was named Young Aerospace Engineer of the Year by AIAA, and garnered the Fulbright Foundation Senior Scholar Lecturing and Research Fellowship, the Institute of Advanced Study Natural Sciences and Technology Fellowship, the Outstanding International Collaboration Award from the Industrial Technology Research Institute of Taiwan, and the Presidential Early Career Award for Scientists and Engineers from the United States White House. He was honored with the 2006 IEEE Eric E. Sumner Award "for pioneering contributions to ultra-wide band communications science and technology." Professor Win is an IEEE Distinguished Lecturer and elected Fellow of the IEEE, cited "for contributions to wideband wireless transmission."